

COMPARISON OF SORPTION CAPACITIES OF HYDROCARBONS ON DIFFERENT
SAMPLES OF MCM-41

A THESIS SUBMITTED TO
THE GRADUATE SCHOOL OF NATURAL AND APPLIED SCIENCES
OF
MIDDLE EAST TECHNICAL UNIVERSITY

BY

BİRSU AYDOĞDU

IN PARTIAL FULFILLMENT OF THE REQUIREMENTS FOR THE DEGREE OF
MASTER OF SCIENCE
IN
CHEMICAL ENGINEERING

FEBRUARY 2013

Approval of the thesis:

**COMPARISON OF SORPTION CAPACITIES OF HYDROCARBONS ON DIFFERENT
SAMPLES OF MCM-41**

submitted by **BİRSU AYDOĞDU** in partial fulfillment of the requirements for the degree of
**Master of Science in Chemical Engineering Department, Middle East Technical
University** by,

Prof. Dr. Canan ÖZGEN _____
Dean, Graduate School of **Natural and Applied Sciences**

Prof. Dr. Deniz ÜNER _____
Head of Department, **Chemical Engineering**

Prof. Dr. Hayrettin YÜCEL _____
Supervisor, **Chemical Engineering Dept., METU**

Prof. Dr. Gürkan KARAKAŞ _____
Co-supervisor, **Chemical Engineering Dept., METU**

Examining Committee Members:

Assoc. Prof. Naime Aslı SEZGİ _____
Chemical Engineering Dept., METU

Prof. Dr. Hayrettin YÜCEL _____
Chemical Engineering Dept., METU

Prof. Dr. Gürkan KARAKAŞ _____
Chemical Engineering Dept., METU

Dr. Cevdet ÖZTİN _____
Chemical Engineering Dept., METU

Assoc. Prof. Burcu Akata KURÇ _____
Nanotechnology Nanobiotechnology Research Center, METU

Date: 01.02.2013

I hereby declare that all information in this document has been obtained and presented in accordance with academic rules and ethical conduct. I also declare that, as required by these rules and conduct, I have fully cited and referenced all material and results that are not original to this work.

Name, Last name: Birsu AYDOĞDU

Signature :

ABSTRACT

COMPARISON OF SORPTION CAPACITIES OF HYDROCARBONS ON DIFFERENT SAMPLES OF MCM-41

AYDOĞDU, Birsu
M. Sc., Department of Chemical Engineering
Supervisor: Prof. Dr. Hayrettin YÜCEL
Co-Supervisor: Prof. Dr. Gürkan KARAKAŞ

January 2013, 69 pages

MCM-41 (Mobil Composition Matter-41) is one of the three members of M41S family and has a highly ordered hexagonal honeycomb like structure with a narrow pore size distribution in mesopore range, high surface area, high pore volume and high thermal stability. These features make MCM-41 proper to use for adsorption, catalysis, ion exchange and separation processes.

In this study sorption capacities of C₈ aromatics (o-, m-, p-xylene and ethylbenzene at 30 °C, 50 °C and 65 °C) on a MCM-41 sample synthesized in our laboratory were determined gravimetrically by using a commercial automated electro balance system and compared with results obtained in a previous and similar MSc thesis study with a sample of different origin and characteristics; specifically low BET surface area (492 m²/g).

MCM-41 sample was synthesized by hydrothermal synthesis method with cetyltrimethylammoniumbromide (CTAMBr as surfactant) and tetraethyl ortosilicate (TEOS as silica source) in basic conditions. This MCM-41 sample was calcined at 540 °C for 8 h and characterized by XRD, nitrogen adsorption at 77 K, TGA, TEM, SEM and SEM-EDX. According to XRD data, main characteristic peak for synthesized MCM-41 was obtained at 2θ=2.28°. Three small reflection peaks can be seen at 2θ values of 2.59, 4.27° and 4.5°. XRD pattern of the MCM-41, indicated that the desired structure of MCM-41 was successfully synthesized. Surface area, pore volume and average pore diameter were obtained from the nitrogen adsorption data at 77 K as 1154 m²/g, 1.306 cm³/g and 2.75 nm respectively. TGA analysis showed that the 540 °C is proper for the calcination. SEM -EDX analysis gave an oxygen atomic concentration 66.40% and silicon atomic concentration 33.60%. These results showed that the chemical composition of the synthesized material was in almost pure SiO₂ form.

The adsorbed amount for all isomers at the same pressure decreased as the temperature of the adsorption isotherms increases as expected for physical adsorption. Nitrogen adsorption of MCM-41 in this study showed type IV isotherm with H2 type hysteresis loop according the IUPAC classification. However, for o-, m-, and p-xylene an approximately linear increase in the adsorbed amount as a function of relative pressure was observed from the adsorption isotherms. Except for adsorption isotherms of m-xylene and p-xylene at 65 °C all isotherms of xylenes showed hysteresis loops. Hysteresis loops narrowed down with increasing temperature. p-xylene and m-xylene adsorption isotherms at 65 °C were reversible and did

not show any hysteresis loop. Ethylbenzene adsorption isotherms at 30 °C, 50 °C and 65 °C also showed a linear increase in the adsorption amount as a function of relative pressure like xylenes. At 50 °C and 65 °C adsorption isotherms of ethylbenzene were reversible without a hysteresis loop. For all adsorbates volume of adsorbed amounts were calculated on the assumption that they exist as saturated liquids at the isotherm temperature and found to be significantly lower than pore volume obtained from nitrogen adsorption isotherm at 77K. Sorption capacities of these hydrocarbons on MCM-41 were also very low when compared to values found in a previous study which involved a MCM-41 sample of significantly lower surface area (492 m²/g). This may be attributed to structure degradation which requires further investigation.

Key-words: MCM-41, Adsorption, Xylenes, Ethylbenzene, Characterization of MCM-41

ÖZ

HİDROKARBONLARIN FARKLI MCM-41 ÖRNEKLERİ ÜZERİNDEKİ SORPSİYON KAPASİTELERİNİN KARŞILAŞTIRILMASI

AYDOĞDU, Birsu
Yüksek Lisans, Kimya Mühendisliği Bölümü
Tez Yöneticisi: Prof. Dr. Hayrettin YÜCEL
Ortak Tez Yöneticisi: Prof. Dr. Gürkan KARAKAŞ

Ocak 2013, 69 sayfa

MCM-41, M41S ailesinin üç üyesinden biridir ve mezo gözenek aralığında dar gözenek boyutu dağılımlı düzgün dağılmış, altıgen peteğe benzer yapıya, yüksek yüzey alanına, yüksek gözenek hacmine ve yüksek termal kararlılığa sahiptir. Bu özellikleri, MCM-41'i adsorpsiyon, katalizör, iyon değişimi ve ayırma işlemleri için kullanılmaya uygun yapmaktadır.

Bu çalışmada, bizim laboratuvarlarımızda sentezlenmiş MCM-41 üzerinde C₈ aromatiklerinin (o-,m-,p-ksilen 30 °C, 50 °C ve 65 °C'de ve etilbenzen 50 °C'de) adsorpsiyon kapasiteleri, gravimetrik olarak ticari otomatikleştirilmiş elektrikli terazi sistemiyle elde edilmiştir ve farklı kaynaklı ve farklı özelliklere; özellikle düşük BET yüzey alanına (492,2 m²/g) sahip örneklerle daha önceden yapılmış benzer Yüksek Lisans çalışmasından elde edilmiş sonuçlarla karşılaştırılmıştır.

Bu çalışmadaki MCM-41 örneği hidrotermal sentez yöntemiyle CTAMBr ve TEOS ile bazik ortamda sentezlenmiştir. Bu MCM-41, 540 °C'de 8 saat kalsine edilmiş ve XRD, 77 K'de nitrojen adsorpsiyonu, TGA, TEM, SEM ve SEM-EDX kullanılarak karakterize edilmiştir. XRD desenine göre ana karakteristik pik 2θ=2,28°'de elde edilmiştir. Üç küçük yansıma piki yaklaşık olarak 2θ 2,59, 4,27° ve 4,5°'dayken görülmüştür. XRD'den elde edilen keskin pik ve yansıma pikleri istenen MCM-41 yapısının başarıyla sentezlendiğini göstermektedir. Yüzey alanı, por hacmi ve ortalama pore çapı 77 K'de azot adsorpsiyon verilerinden sırasıyla 1154 m²/g, 1,306 cm³/g ve 2,75 nm olarak bulunmuştur. TGA analizi 540 °C'nin kalsinasyon için uygun olduğunu göstermiştir. SEM-EDX analizinden elde edilen atomik analize göre oksijenin atomik konsantrasyonu %66,40 silisyumun atomik konsantrasyonu %33,60 olarak bulunmuştur. Bu sonuçlar sentezlenen malzemenin saf SiO₂ formunda olduğunu gösterir.

Aynı basınçta adsorplanan miktar tüm izomerler için, fiziksel adsorpsiyondan beklendiği gibi adsorpsiyon izoterm sıcaklığı yükseldikçe düşmüştür. Bu çalışmadaki MCM-41 üzerinde nitrojen adsorpsiyonu IUPAC sınıflandırmasına göre H2 türünde histeresiz ile tip IV özellikleri göstermiştir. Fakat o-, m-, p-ksilen için adsorpsiyon izotermelerinde göreceli basınç fonksiyonu olarak adsorplanan miktarı yaklaşık olarak lineer artmıştır. 65 °C'de ki p-ksilen ve m-ksilen adsorpsiyon izotermelerinin dışında tüm izotermeler histeresiz eğrileri göstermiştir. Histeresiz eğrileri yükselen sıcaklıkla daralmıştır. 65 °C'de p-ksilen ve m-ksilen adsorpsiyon izotermeleri geri dönüşümlüdür histeresiz eğrisi göstermemiştir. 30 °C, 50 °C ve 65 °C'de etilbenzen adsorpsiyon izotermelerinde de ksilenler gibi göreceli basınç fonksiyonu olarak adsorplanan miktar lineer artış göstermiştir. 50 °C ve 65 °C'de ki etilbenzen izotermeleri geri dönüşümlüdür, histeresiz eğrisi göstermez. Tüm adsorbatlar için adsorplanan hacim izoterm sıcaklığında doygun sıvı olduğu kabul edilerek hesaplanmıştır ve 77 K'de nitrojen adsorpsiyonundan elde edilen gözenek hacmiyle karşılaştırıldığında oldukça düşüktür. Bu hidrokarbonların MCM-41 üzerindeki adsorpsiyon kapasiteleri, daha düşük yüzey alanı

(492,2 m²/g) olan MCM-41 ieren daha nceki alıřmayla karřılařtırıldıđında ok dřktr. Bu durum daha ileri arařtırmaları gerektiren MCM-41 rneđinin yapısındaki bozulmadan kaynaklanıyor olabilir.

Anahtar Kelimeler: MCM-41, Adsorpsiyon, Ksilenler, Etilbenzen, MCM-41 karakterizasyonu

To my mother...

ACKNOWLEDGEMENT

I would like to express my deepest thanks and gratitude to Prof. Dr. Hayrettin YÜCEL for his supervision and for his patience against all difficulties we met through this study.

I would like to thank to my co-supervisor Prof.Dr. Gürkan KARAKAŞ, for his crucial advises to overcome the problems and suggestions.

I would like to thank to my friend Seval Gündüz, for sharing her experience about synthesis steps of MCM-41 and for her help to synthesize MCM-41 which is used as my sample in my experiments.

I would like to thank to Prof. Dr. Timur DOĞU, for his permission to use his laboratory chemicals and equipments.

I would like to thank to Assoc. Prof. Naime Aslı SEZGİ, for the sample supports and for giving information about synthesis steps of MCM-41

I would also like to thank to my friend Özgen YALÇIN for her support, help and crucial advises for my thesis.

I would like to thank my friends Gülen Göktürk and Mine Toker. They gave me motivation and visited me with a birthday cake when I was working in the laboratory.

I would like to cherish my friend Baraa Abbas Ali. He thought me how to use IGA system.

I would like to thank my co-workers İrem Ocakcioğlu, Pınar Şimşek, Tuğçe İlhan, Zeynep Hatipoğlu, Seda Baykal, Evrim Göz, Dursun Güngören for their motivation and support when I was working at school or dealing with problems.

I would also like to thank my supervisors at work Faruk Birsen and Erensoy Topçu. They let me go to school whenever I asked during the working hours despite of the workload.

Special thanks go to my mother Sultan AYDOĞDU and my uncle Hüseyin HAZER for always being there to help me and giving me the motivation.

TABLE OF CONTENTS

ABSTRACT	v
ÖZ	vii
ACKNOWLEDGEMENT	x
TABLE OF CONTENTS	xi
LIST OF TABLES	xiii
LIST OF FIGURES	xiv
NOMENCLATURE	xv
CHAPTERS	
1 INTRODUCTION	1
1.1. Porous Materials	2
1.2. M41S Family	3
1.2.1. MCM-41	4
1.2.2. MCM-48	5
1.2.3. MCM-50	6
1.3. Synthesis of M41S Family and MCM-41	6
1.3.1. MCM-41 Synthesis Components	7
1.4. Formation Mechanisms of MCM-41	8
1.4.1. Liquid Crystal Templating (LCT) Mechanism	8
1.4.2. Transformation Mechanism from Lamellar to Hexagonal Phase	9
1.5. Characterization Techniques for MCM-41 Type of Materials	10
1.5.1. X-Ray Diffraction (XRD)	10
1.5.2. Nitrogen Physisorption at 77 K	11
1.5.3. Transmission Electron Microscopy (TEM)	11
1.5.4. Thermal Gravimetric Analysis (TGA)	11
1.6. Applications of MCM-41	11
1.7. Adsorption on Porous Materials	12
1.8. Aim of This Study	14
2 LITERATURE SURVEY	15
3 EXPERIMENTAL	19
3.1. MCM-41 Synthesis Procedure	19
3.2. Investigation of Adsorption Isotherms	20
3.2.1. Intelligent Gravimetric Analyzer (IGA)	20
3.2.2. Experimental Procedure	23
4 RESULTS AND DISCUSSION	29
4.1. Characterization of MCM-41	29

4.1.1. X-Ray Diffraction (XRD) Analysis	29
4.1.2. Nitrogen Physisorption Analysis	30
4.1.3. TGA Analysis	32
4.1.4. TEM Analysis	33
4.1.5. SEM Analysis.....	34
4.1.6. EDX Analysis	35
4.2. Adsorption of p-xylene, m-xylene, and o-xylene on MCM-41	35
4.3. Adsorption of Ethylbenzene on MCM-41	43
5 CONCLUSION AND RECOMMENDATIONS	47
REFERENCES	49
APPENDICES	
A ANTOINE EQUATION AND COEFFICIENTS	53
A.1 Antoine Equation	53
B ADSORPTION ISOTHERMS DATA FOR ALL SORBATES	55
B.1. Adsorption Isotherms Data for o-,m-,p-xylene.....	55
B.2. Adsorption Isotherms Data for Ethylbenzene	60
C ADSORPTION ISOTHERMS DATA OF PREVIOUS STUDY OF C ₈ AROMATICS ON MCM-41	63
C.1. Nitrogen adsorption at 77 K.....	63
C.2. Equilibrium sorption capacities of C ₈ aromatics on MCM-41	64
D INTELLIGENT GRAVIMETRIC ANALYZER.....	65
D.1. Intelligent gravimetric analyzer (IGA system).....	65
D.1.1. IGA-001- Gas Sorption System.....	65
D.1.2. IGA-002 – Vapor Sorption System.....	65
D.1.3. IGA-003 –Dynamic Sorption System	65
D.2. Sample Loading.....	65
D.2.1. Gas Setup Tool	66
D.2.2. New Application Tool	66

LIST OF TABLES

TABLES

Table 1.1: Pore sizes of MCM-41 synthesized with different surfactants	8
Table 3.1: Grades and origins of sorbates.....	26
Table 4.1: Surface area, pore volume, and BJH desorption pore diameter of MCM-41 sample	31
Table 4.2: Elemental EDX analysis of MCM-41.....	35
Table 4.3: Kinetic diameters of xylenes	36
Table 4.4: Equilibrium sorption capacities of p-xylene.....	40
Table 4.5: Equilibrium sorption capacities of m-xylene.....	40
Table 4.6: Equilibrium sorption capacities of o-xylene.....	41
Table 4.7: Sorption capacities of p-xylene at similar pressure values.....	41
Table 4.8: Sorption capacities of m-xylene at similar pressure values.....	41
Table 4.9: Sorption capacities of o-xylene at similar pressure values.....	41
Table 4.10: The adsorbed volumes (V_p) of p-xylene	42
Table 4.11: The adsorbed volumes (V_p) of m-xylene	42
Table 4.12: The adsorbed volumes (V_p) of o-xylene	42
Table 4.13: Equilibrium sorption capacities of ethylbenzene.....	43
Table 4.14: The adsorbed volumes (V_p) of ethylbenzene.....	45
Table A.1: Antoine coefficient for the sorbates	53
Table A.2: Vapor pressure of sorbates at adsorption temperatures (calculated by Antoine equation)	53
Table B.1: Adsorption isotherm data for p-xylene at 30°C	55
Table B.2: Adsorption isotherm data for p-xylene at 50°C	55
Table B.3: Adsorption isotherm data for p-xylene at 65°C	56
Table B.4: Adsorption isotherm data for m-xylene at 30°C	57
Table B.5: Adsorption isotherm data for m-xylene at 50°C	57
Table B.6: Adsorption isotherm data for m-xylene at 65°C	58
Table B.7: Adsorption isotherm data for o-xylene at 30°C	58
Table B.8: Adsorption isotherm data for o-xylene at 50°C	59
Table B.9: Adsorption isotherm data for o-xylene at 65°C	59
Table B.10: Adsorption isotherm data for ethylbenzene at 30°C.....	60
Table B.11: Adsorption isotherm data for ethylbenzene at 30°C (2 nd run)	61
Table B.12: Adsorption isotherm data for ethylbenzene at 50°C.....	61
Table B.13: Adsorption isotherm data for ethylbenzene at 65°C.....	62
Table C.1: Equilibrium sorption capacities of p-xylene	64
Table C.2: Equilibrium sorption capacities of m-xylene	64
Table C.3: Equilibrium sorption capacities of o-xylene	64
Table C.4: Equilibrium sorption capacities of ethylbenzene	64
Table D.1: IGA-002 valve position for static mode gas pressure set (Idle mode)	68

LIST OF FIGURES

FIGURES

Figure 1.1: Classification of porous materials according to their pore diameter ranges	3
Figure 1.2: The M41S family of materials including MCM-41, MCM-48 and MCM-50	4
Figure 1.3: Surfactant behavior in water-surfactant binary system	4
Figure 1.4: (a) Schematically representation of MCM-41 (b) TEM image of MCM-41	5
Figure 1.5: Schematic representation of 3-D cubic structure of MCM-48	6
Figure 1.6: Schematic representation of MCM-50 lamellar structure	6
Figure 1.7: Schematic representation of typical surfactant	7
Figure 1.8: The schematic model of LCT mechanism with two possible pathways	9
Figure 1.9: Schematic model for transformation mechanism from lamellar to	10
Figure 1.10: IUPAC classification types of adsorption isotherms	13
Figure 1.11: Types of hysteresis loops	14
Figure 3.1: Synthesis steps of MCM-41	20
Figure 3.2: IGA system	21
Figure 3.3: IGA-002 configuration set for vapor sorption operation (Idle mode)	22
Figure 3.4: Experimental procedure steps of adsorption isotherm data	23
Figure 3.5: Lowering the sample reactor	24
Figure 3.6: Loading sample container (pan)	24
Figure 3.7: Manual vacuum valve	25
Figure 3.8: Liquid reservoir	25
Figure 3.9: Temperature setup window	27
Figure 3.10: Isotherm setup window	27
Figure 4.1: XRD pattern of MCM-41	30
Figure 4.2: Nitrogen physisorption isotherm of synthesized MCM-41	31
Figure 4.3: BJH desorption pore size distribution of MCM-41	32
Figure 4.4: TGA analysis of uncalcined MCM-41	32
Figure 4.5: TEM images of MCM-41	33
Figure 4.6: SEM images of MCM-41	34
Figure 4.7: EDX analysis of MCM-41	35
Figure 4.8: Adsorption isotherm of p-xylene at 30 °C	36
Figure 4.9: Adsorption isotherm of p-xylene at 50 °C	36
Figure 4.10: Adsorption isotherm of p-xylene at 65 °C	37
Figure 4.11: Adsorption isotherm of m-xylene at 30 °C	37
Figure 4.12: Adsorption isotherm of m-xylene at 50 °C	38
Figure 4.13: Adsorption isotherm of m-xylene at 65 °C	38
Figure 4.14: Adsorption isotherm of o-xylene at 30 °C	39
Figure 4.15: Adsorption isotherm of o-xylene at 50 °C	39
Figure 4.16: Adsorption isotherm of o-xylene at 65 °C	40
Figure 4.17: Adsorption isotherm of ethylbenzene on MCM-41 at 30 °C	43
Figure 4.18: Adsorption isotherm of ethylbenzene on MCM-41 at 50 °C	44
Figure 4.19: Adsorption isotherm of ethylbenzene on MCM-41 at 65 °C	44
Figure C.1: Nitrogen adsorption at 77 K on MCM-41 in previous study	63
Figure C.2: BJH adsorption pore size distribution of MCM-41 in previous study	63

NOMENCLATURE

MCM	Mobil Composition Matter
CTMABr	Cetyltrimethylammoniumbromide
TEOS	Tetraethyl orthosilicate
IUPAC	International Union of Pure and Applied Chemistry
IGA	Intelligent Gravimetric Analyzer
XRD	X-Ray Diffraction
TGA	Thermal Gravimetric Analysis
TEM	Transmission Electron Microscopy
SEM	Scanning Electron Microscopy
EDX	Energy Dispersive Spectroscopy
d_{100}	Interplanar spacing value
a	Distance between pore centers
b_d	Wall thickness
w_d	Pore diameter
P	Pressure at any time (mbar)
P_o	Saturation vapor pressure at temperature of isotherm (mbar)
Wt	Weight at any time
Wto	Weight of adsorbent at initial time

CHAPTER 1

INTRODUCTION

Over the past 50 years, for catalysis, adsorption, separation and environmental pollution control processes design, synthesis, characterization and property assessment of zeolites and molecular sieves are studied. [1] Due to demands of industrial and fundamental studies there has been a growing interest in expanding pore sizes of zeotype materials from the micropore region to mesopore region. The separation of heavy metal ions, the separation and selective adsorption of large organic molecules from waste water, the formation of a supramolecular assembly of molecular arrays, the encapsulation of metal complexes in the frameworks, and the introduction of nanometer particles for electronic and optical applications are the examples which cause needs to larger pores than micropores. As a result of these demands a significant amount of work to create zeotype materials with pore diameters larger than those of the traditional zeolites were carried out [2].

In 1992, Mobil Oil Corporation scientists synthesized a new family of molecular sieves which is called M41S family [3]. This type of ordered mesoporous materials consist of MCM-41, MCM-48 and MCM-50 [4]. MCM-41 has attracted more attention of scientist since it has high surface area, high thermal and hydrothermal stability, controllable pore size, hydrophobicity and acidity. This porous material composed of hexagonally arranged channels with pore diameters varying from 1.5 to 10 nm. These features of this material make it a promising material as catalyst and support and can be usable in the industry for adsorption, ion exchange and environmental control [3].

MCM-41 has received a great attention in the area of separation and adsorption. The uniform pore structure within the mesopore range and the high pore volume makes MCM-41 usable for separations that vary from the removal of organic and inorganic contaminants in waste streams to chromatographic media. MCM-41 have been characterized by investigation adsorption of several molecules such as nitrogen, oxygen, water, cyclopentane, toluene, and carbon tetrachloride, and alcohols [5,6]. These early works demonstrated the extraordinary high sorption capacity of MCM-41 for hydrocarbons such as benzene compared to that of the classical microporous molecular sieves [7].

Xylene isomers and ethylbenzene are the aromatic compounds obtained from petroleum. Xylene is referring to the three isomers o-xylene, m-xylene, and p-xylene. Isomers have similar physicochemical properties therefore the process of producing pure isomers is complicated. Pure xylenes are used as raw materials in the plastic and rubber industries. The use of these products with high levels of purity enhances process efficiency and decreases the costs. Therefore separation of C₈ aromatic takes attention. For the separation of C₈ aromatics according to kinetic diameter of the substances molecular sieves can be used. The selective adsorption on zeolite is commonly considered to be the most economical way in the industrial process for the separation [8,9]. Studies showed that medium-pore channels were excellent for the separation of p-xylene and ethylbenzene from C₈ aromatics. Therefore adsorption of C₈ aromatics on MCM-41 was investigated.

In this study, a MCM-41 type of mesoporous molecular sieve was synthesized to be used as adsorbent by using CTAMBr as surfactant and TEOS as silica source. Synthesized MCM-41 was characterized by XRD, nitrogen adsorption at 77 K, TEM, SEM, EDX and TGA. Sorption

capacities of p-xylene, m-xylene and o-xylene on this sample were investigated gravimetrically with an automated gravimetric electrobalance system (IGA, HIDEN) by determining adsorption isotherms at different temperatures which are 30 °C, 50 °C and 65 °C. To observe also sorption capacity of the ethylbenzene on synthesized MCM-41 isotherm data was obtained at 30 °C, 50 °C and 65 °C.

In this chapter, porous materials especially M41S family members are summarized and background information about these materials is given.

In Chapter 2, literature survey about the MCM-41 and adsorption on the MCM-41 type of molecular sieves are given.

In Chapter 3, experimental procedure of MCM-41 synthesis and adsorption measurements are described. Besides, information about the experimental set up is given in this chapter.

In Chapter 4, characterization results of MCM-41 are given. Obtained sorption isotherm data of p-xylene, m-xylene and o-xylene on this synthesized MCM-41 at 30 °C, 50 °C and 65 °C and ethylbenzene sorption capacity at 50 °C are given and discussed. Finally, conclusions and recommendations are displayed in Chapter 5.

1.1. Porous Materials

Porous materials are used in chemical reactions and industrial applications as adsorbents, ion exchangers, catalyst and catalyst supports [10,11]. Porous materials classified into three types according to IUPAC (International Union of Pure and Applied Chemistry) definition:

1) Microporous materials: Pore diameters of these materials are less than 2 nm. The most widely used microporous materials are zeolites. In addition to zeolites, other members of microporous materials are pillared clays, some metal phosphates like titanium, zirconium etc., amorphous silica, inorganic gels and carbon molecular sieves [10, 12].

2) Mesoporous materials: Pore diameters of these materials are between 2-50 nm [10]. Silica and alumina are examples of mesoporous materials. The pores of alumina and silica are irregularly arranged. Regularly arranged members are MCM-41 (hexagonal), MCM-48 (cubic) and MCM-50 (lamellar) [11,13].

3) Macroporous materials: Pore diameters are greater than 50 nm [10]. Porous glasses and alumina membrane are members of macroporous materials [12].

The most widely used members of the microporous materials are zeolites. They are crystalline aluminosilicates molecular sieves materials which has a narrow size distribution [1,14]. They became extremely successful as catalyst due to these features:

- Very high surface area and adsorption capacity
- Controllable adsorption properties (vary from hydrophobic to hydrophilic type materials),
- Generation of active acid sites in the framework and adjustable strength and concentration for a particular application
- Uniform structure of channels, that let zeolites to present different types of shape selectivity such as product, reactant and transition state,
- Usable to direct a given catalytic reaction towards the desired product without the side reactions [14]
- Thermal and hydrothermal stability which are necessary to be used as catalyst [15]

Although zeolites have these advantages listed above, they have one serious limitation. They are not being able to process molecules larger than their pore diameters which are maximum 1-1.2 nm [15]. Therefore, to overcome this limitation researches are made to

increase zeolites diameter to the mesoporous region by maintaining the crystalline structure. For this purpose, in the early 1980s at Union Carbide, AlPO_4 structures having a pore size range of 1.3-1.5 nm was discovered. After discovery of AlPO_4 , related materials such as SAPO's (silicoaluminophosphates) and MeAPOs (metal aluminophosphates) were synthesized [15]. The common problems of these materials are they are not thermally and hydrothermally stable.

In 1990, Yanagisawa reported the syntheses of ordered mesoporous materials with narrow pore size distribution and large surface area [16]. These materials were prepared from the layered polysilicate which is named as kanemite. In 1992, Mobil Oil Corporation researchers discovered a group of mesoporous materials. These materials have narrow size distributions, large surface area and tunable from 1.5 nm to 10 nm and called M41S family. These materials differ from the zeolites with their amorphous pore walls [14]. It was a breakthrough in the history of mesoporous materials [17, 18].

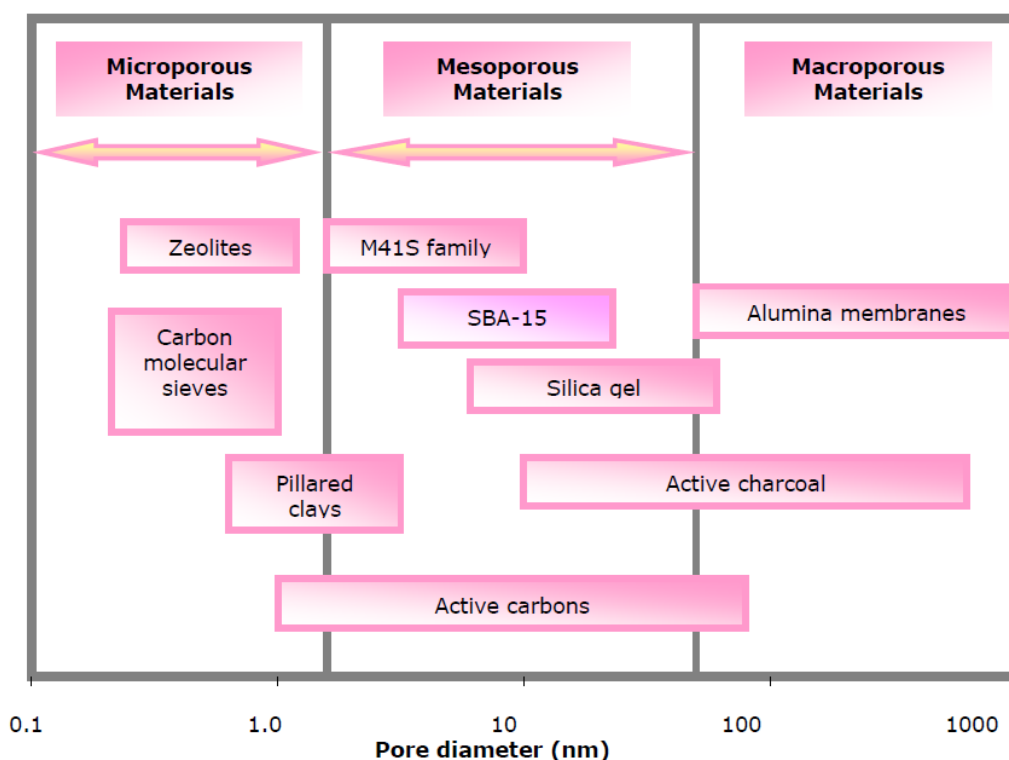


Figure 1.1: Classification of porous materials according to their pore diameter ranges [19]

1.2. M41S Family

A new class of silicate/aluminosilicate molecular sieves with regular arrangements of mesopores was discovered by Mobil Cooperation researchers in 1992. These new mesostructured molecular sieves are called M41S family [20]. In this family three different mesophases have been identified which are, 1-D MCM-41 with hexagonally-ordered pore structure, 3-D MCM-48 with cubic-ordered pore structure and MCM-50 with unstable lamellar structure [21].

This new family of mesoporous material has regularly arranged channels and narrowly distributed pore diameters although it is disordered and amorphous from the atom level [22]. The pore structures of the M41S family three different mesophases are shown in Figure 1.2.

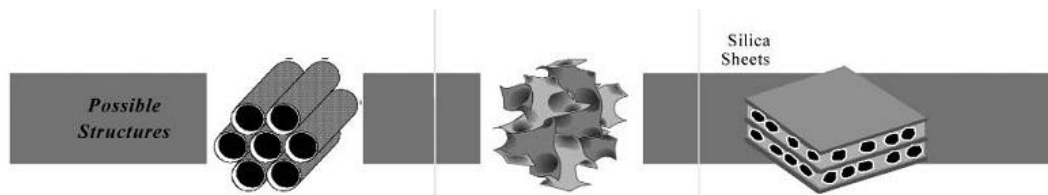


Figure 1.2: The M41S family of materials including MCM-41, MCM-48 and MCM-50 [21]

M41S family materials have unique physical and chemical properties. These ordered mesoporous materials generally, have large surface area, above 1000 m²/g and pore diameters are between 2- 50 nm. Also these materials surfaces have active centers. Therefore their surfaces can be decorated or modified easily [22].

After the discovery of new types of mesoporous materials, researchers tried to understand the detailed mechanism of the synthesis procedure and characterization of these materials. For each member of the M41S family, the synthesis steps are mainly the same. To synthesize M41S, a structure-directing surfactant, a source of silica, a solvent and a catalyst (an acid or a base) are required components. Synthesis of MCM-41, MCM-48 and MCM-50, differs in the ratio of surfactant to silica source. In other words, in water-surfactant binary systems increasing the surfactant concentration varies the formed structure which is seen in Figure 1.3. [10,15,1].

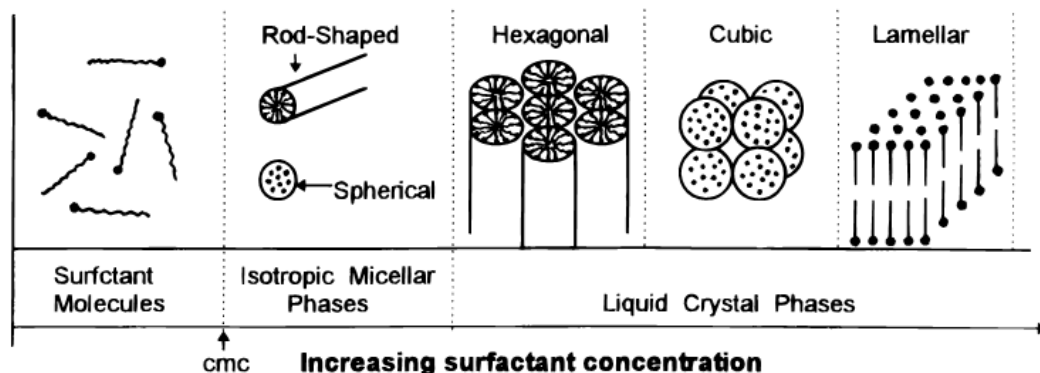


Figure 1.3: Surfactant behavior in water-surfactant binary system [1]

At low concentrations, in water-surfactant binary system surfactants exist as monomolecules. As surfactant concentration continues to increase to decrease the system entropy surfactant molecules aggregate together to form micelles. The lowest concentration, that monomolecules aggregate to form micelles, is called cmc (critical micellization concentration). Hexagonal phases appear with further concentration increase. If concentration of surfactant still increases lamellar phase formation occurs. In some cases, between hexagonal and lamellar phases, cubic phase can form [1].

1.2.1. MCM-41

MCM-41 (Mobil Composition of Matter No.41) is widely used member of M41S family as the other members are either thermally unstable (MCM-50) or hard to obtain (MCM-48). Also it

takes attentions due to its high surface area, high thermal and hydrothermal stability, controllable pore size, its hydrophobicity and acidity [3].

As seen in Figure 1.4, structure of MCM-41 type mesoporous materials, is unique unidirectional, and is like as honeycomb [23]. Their internal surface area is approximately 1000 m²/g, and hexagonally arranged channel diameters vary from 1.5 to 10 nm [3].

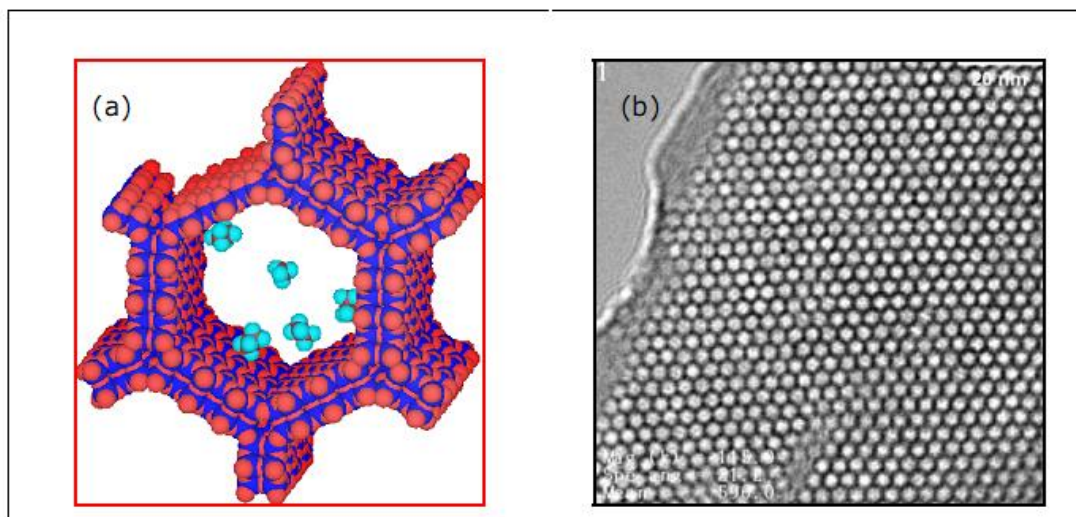


Figure 1.4: (a) Schematically representation of MCM-41 (b) TEM image of MCM-41 [24]

Pore surface of the MCM-41 is heterogeneous because of the hexagonal shape of the pore which can be seen in the figure above. At the corners of the pore enhanced siloxane bridges has been detected. These bridges help to create hydrophobic portions on the pore surface. On the other hand the flat areas of the pore surface are hydrophilic because of the hydroxyl groups [25].

Formation mechanism of the MCM-41 takes more attentions of researches. As a result of the studies about formation mechanism, two mechanisms have been proposed. One of the mechanisms is liquid crystal templating (LCT) mechanism proposed by Beck et al [20]. The other formation mechanism is transformation mechanism from lamellar to hexagonal phase which was proposed by Stucky et al [26]. These mechanisms are explained in following sections.

1.2.2. MCM-48

MCM-48 has a 3-D cubic structure which is shown in Figure 1.5. In addition to high thermal stability characteristic, MCM-48 has interesting properties such as it has a high specific surface area up to 1600 m²/g and pore volume up to 1.2 cm³/g. Interwoven and branched pore structure of MCM-48 makes it more proper to mass transfer kinetics in catalytic and separation applications [27]. MCM-48 is not widely used because its synthesis methods have some difficulties and they are not reproducible. Also these methods are costly. These disadvantages limit the availability of MCM-48 type of mesoporous materials. [28].

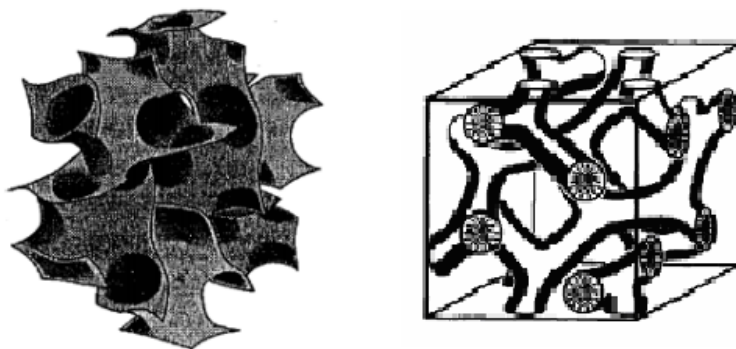


Figure 1.5: Schematic representation of 3-D cubic structure of MCM-48 [Adapted from 29 and 6]

1.2.3. MCM-50

MCM-50 is the members of M41S family which has a non-stable lamellar structure. This non-stable structure stabilized by post synthesis treatment that is calcination and does not give a mesoporous compound [11,30]. The schematic representation of MCM-50 structure is shown in Figure 1.6.

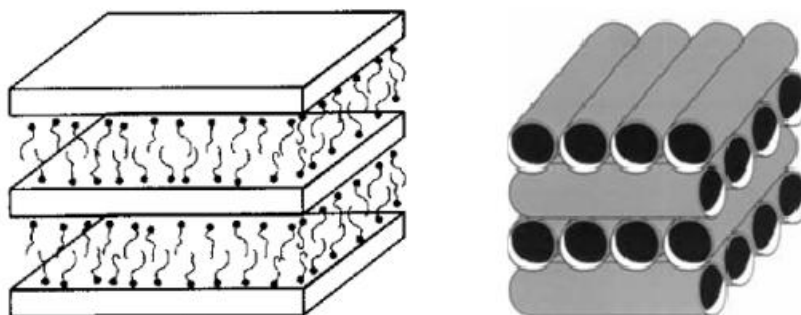


Figure 1.6: Schematic representation of MCM-50 lamellar structure [Adapted from 30]

1.3. Synthesis of M41S Family and MCM-41

For each members of the M41S family, the synthesis steps are mainly the same. To synthesize M41S, a structure-directing surfactant, a source of silica, a solvent and a catalyst (an acid or a base) are required components [15].

M41S family mesoporous materials are synthesized by polymerizing a silica source around an organic template in an aqueous solvent. These mesoporous materials contains high amount of organic material due to their organic templates. After the pore formation, hydrothermal post-synthesis treatment is applied to empty the pores and the organic template is removed by calcination [15,21,25,31].

The particular phase (hexagonal, cubic or lamellar) present in a surfactant aqueous solution depends on the surfactant concentration [1]. According to Myers et al, the interaction between the organic template molecules and the silicate framework also forms phase. This interaction is influenced by the synthesis parameters and nature of itself [32].

The Mobil researchers found that relative concentrations of the species present in the synthesis solutions affect the final pore structures. The diameter of the pores can be controlled by changing the length of template molecule. Moreover, changing the silica sources, surfactants, auxiliary compounds or reaction conditions like solvent, temperature, aging time, reactant mole ratio and pH of the medium provides the production of new mesoporous systems. These changes also affect the thermal, hydrothermal and mechanical stabilities of the materials. Hence, to obtain the optimum conditions for the synthesis of MCM-41, researchers studied modified MCM-41 synthesis [17,18,33,34].

1.3.1. MCM-41 Synthesis Components

In MCM-41 synthesis required components are the same with other M41S family members. A template (a surfactant), a source of silica, a solvent and a mineralizing agent (an acid or a base) are the synthesis components of MCM-41[15].

1.3.1.1. Surfactants

The term surfactant is the short form of “surface active agent” and refers to a class of chemical compounds known as amphiphiles which comes from two Greek words meaning they are not certain what they like. Surfactants composed of two parts as shown in Figure 1.7: One part is polar (dipole or charged group), and the other part is non-polar (usually a hydrocarbon or halocarbon chain). The polar part is hydrophilic and the non-polar part is hydrophobic, hence the molecule self-organizes itself in water in such a way as to minimize contact between incompatible ends [35,36].

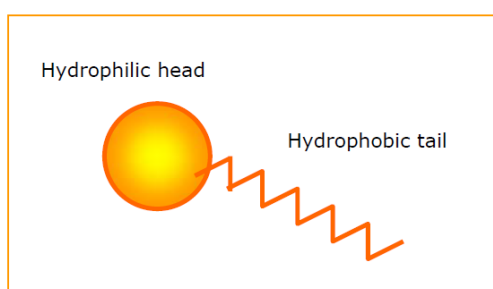


Figure 1.7: Schematic representation of typical surfactant [24]

For the synthesis of MCM-41 ionic surfactants such as cetyltrimethylammonium bromide (CTMABr, $C_{16}H_{33}(CH_3)_3NBr$), cetyltrimethylammonium chloride (CTMACl) are the most commonly used templating agents. In general, the use of low-molecular-weight amphiphiles with the formula $C_nH_{2n+1}(CH_3)_3N^+$ ($n = 8-22$) or $C_nH_{2n+1}C_5H_5N^+$ ($n = 12$ or 16) result in the formation of MCM-41. The formation mechanism of MCM-41, by using these surfactants, is based on the electrostatic interactions between the positively charged surfactants and negatively charged silicate species in solution [12].

By changing the surfactant alkyl chain length in MCM-41 synthesis, the pore size of the MCM-41 can be modified in the range of 2-5 nm. Different alkyl chain lengths used to observe the effects on the pore size. Some pore diameter values obtained for MCM-41 materials using different surfactants with different alkyl chain lengths listed in the Table 1.1. As seen in the table pore diameters increase with the increasing alkyl chain length.

Table 1.1: Pore sizes of MCM-41 synthesized with different surfactants [17]

Surfactant Chain Length $C_nH_{2n+1}(CH_3)_3N^+$ n=	Average pore size (nm)
8	18
9	21
10	22
12	22
14	30
16	37

1.3.1.2. Silica Sources

In the MCM-41 synthesis sodium silicate (Na_4O_4Si), sodium meta-silicate (Na_2SiO_3), fumed silica, silica gel and tetraethyl orthosilicate (TEOS) were used as silica sources. Generally MCM-41 synthesized in basic medium, however acidic medium is also used. In synthesis at acidic conditions usually TEOS is used as silica source. Other silica sources are used in synthesis at basic conditions [15].

1.3.1.3. Solvent

Water is used as the solvent in the synthesis of MCM-41. The amount of water added to the synthesis mixture is critical because it determines the properties of the silicate and the surfactant mixture. If the amount of water is less than a certain amount, the precipitation of the MCM-41 crystals becomes difficult because of a compact medium. On the other hand, if too much water used as solvent, the interaction between the surfactant and silicate molecules becomes weaker and it is not possible to produce a gel during the synthesis [12].

1.3.1.4. Mineralizing Agent

The mineralizing agent can be an acid or a base. Mineralizing agents mineralize the silica sources into soluble species with suitable morphologies capable of associating with surfactant molecules to form various periodic mesophases. For this purpose, useable basic agents are sodium hydroxide, tetramethyl ammonium hydroxide or tetraethyl ammonium hydroxide and HCl, HF or HNO_3 are the usable acidic agents [12,15].

1.4. Formation Mechanisms of MCM-41

The formation mechanisms of MCM-41 have attracted much attention. First proposed mechanism is liquid crystal templating (LCT) mechanism [17]. For the LCT formation mechanism a second pathway proposed according to their researches [37]. Later another formation mechanism which is transformation mechanism from lamellar to hexagonal phase was proposed by Stucky et al [1].

1.4.1. Liquid Crystal Templating (LCT) Mechanism

This mechanism is the first proposed mechanism. According to the LCT mechanism, surfactants which act as templates for the formation of MCM-41, defines the structure with their arrangements. The first step in the LCT mechanism is formation of rod-shaped micelles. These micelles act like a template rather than individual single molecules or ions.

Then hexagonal liquid crystal mesophases form and with the addition of silicate species, hexagonal array with silicate layer structure appears. Finally, surfactant is removed by calcination and MCM-41 with cylindrical pores structure is obtained. A second pathway for the LCT mechanism is proposed by Beck et al [17] for the formation of MCM-41. In the second pathway, silicate species interact with randomly ordered rod-shaped micelles and silicate encapsulated micelles form. These randomly ordered composite species spontaneously pack into highly ordered mesoporous phase with hexagonal arrangement. Then again surfactants is removed from the pores by calcination and MCM-41 structure forms [1,17,38]. The schematic model of LCT mechanism with two possible pathways is shown in Figure 1.8.

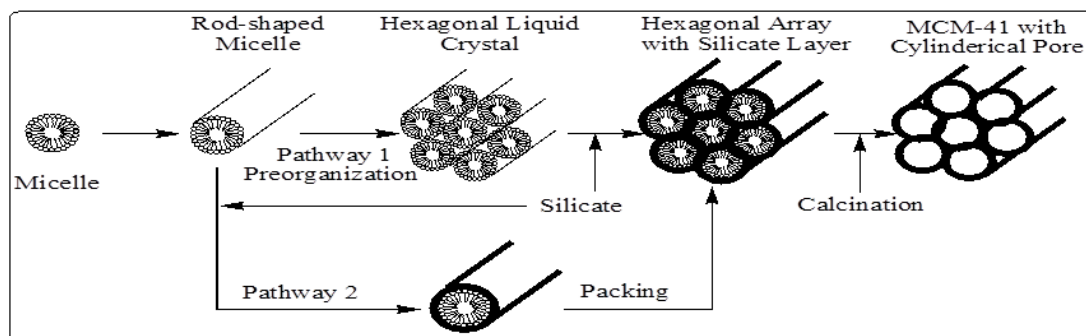


Figure 1.8: The schematic model of LCT mechanism with two possible pathways [2]

Chen et al investigated that the formation mechanism by employing XRD, ^{29}Si NMR, ^{14}N NMR and TGA techniques. No hexagonal liquid crystalline mesophases was detected either in the synthesized gel or in the surfactant solution which was used as template. Therefore, it was concluded that pathway 2 is responsible for the formation of MCM-41 structure. The randomly ordered rod-like organic micelles interact with silica species to form two or three monolayers of silica on the outer surfaces of the micelles. Then these composite species spontaneously self-organize into a long range ordered structure to form the final hexagonal packing mesoporous MCM-41 [1,2,37].

1.4.2. Transformation Mechanism from Lamellar to Hexagonal Phase

According to transformation mechanism from lamellar to hexagonal phase which proposed by Stucky et al.,[38] ion exchange occurs between silicate oligomers and surfactants in the precursor solution in the early stage of the formation. Then surfactant-silica complex is formed and this complex forms a SLC (silicatropic liquid crystal) phase. Before the silicate species condense, a low-curvature lamellar phase is formed because of the highly charged silica species and the charge density matching. The condensation of silicate causes a rearrangement of surfactant that leads mesophase transformation from low-curvature lamellar phase to high-curvature hexagonal phase.[38]. The schematic representation of transformation mechanism for the formation of MCM-41 from aqueous solution of surfactant and silica source is given in Figure 1.9.

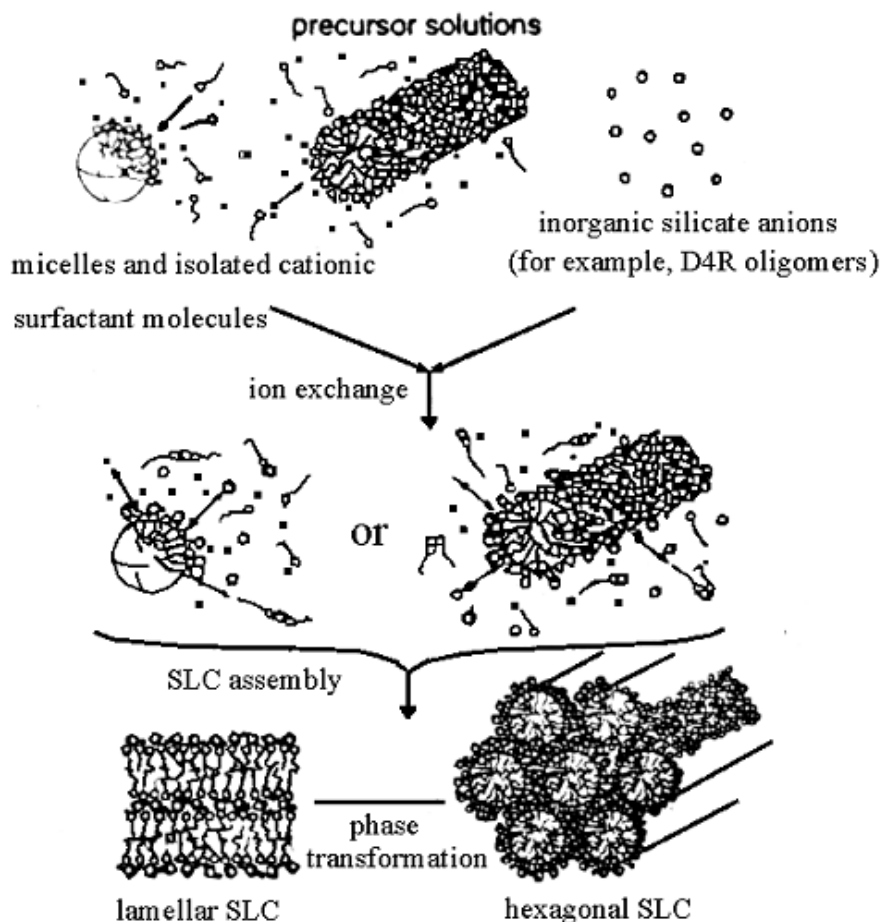


Figure 1.9: Schematic model for transformation mechanism from lamellar to hexagonal phase [38]

1.5. Characterization Techniques for MCM-41 Type of Materials

For MCM-41 type of materials, pre and post synthetic treatment procedures have been studied by several researchers. Effects of these procedures on the variation of surface properties, mesopore size and pore structure were examined by using characterization techniques. For characterization of pores XRD, nitrogen physisorption at 77 K, transmission electron microscopy (TEM), scanning electron microscopy (SEM), and thermo gravimetric analysis (TGA) are the used characterization techniques [39].

1.5.1. X-Ray Diffraction (XRD)

X-ray diffraction is a standard method for characterizing the structure of ordered porous materials. This method is used to determine the crystal structure of a material. This method is very convenient for analyzing the structure of ordered porous materials. For the MCM-41 type of mesoporous material, the XRD peaks come from the well ordered pores, not from crystal structure in the atomic range. A well-ordered, MCM-41 gives a sharp plane diffraction peak (100) and reflection peaks of higher Miller Index planes, (110), (200) and (210). MCM-41 only gives diffraction peaks at the low angle range ($2\theta < 10$). This situation shows that pore

walls of these types of mesoporous materials are mainly amorphous. However, the surfaces of the pore walls show crystalline-like behavior [40].

1.5.2. Nitrogen Physisorption at 77 K

Low-temperature nitrogen physisorption is a standard procedure to determine surface area and pore size distribution for porous materials. For the characterization of porous material, physisorption measurement is done at constant temperature of 77 K. Characteristic of the isotherm shape gives information about nature of the gas-adsorbent interaction, surface area and porosity of the adsorbent. MCM-41 materials have uniform pores ranging from 1.5 to 10 nm [41].

Nitrogen physisorption (adsorption) isotherm of MCM-41 shows a sharp step in the mesoporous range of $P/P_0 = 0.2$ to 0.5 which indicates the liquid condensation of N_2 at 77 K in the uniform mesopores of MCM-41 [41].

1.5.3. Transmission Electron Microscopy (TEM)

Transmission electron microscopy (TEM) is a standard method to characterize the ordered structure of materials. In this method, a high energy beam (100-200 kV) is used to image a thin material specimen. The high-energy electron beam transmits the sample grids and casts an image of the sample's structure. According to TEM analysis the shape of the pore channels of MCM-41 is hexagonal. [24,66]

1.5.4. Thermal Gravimetric Analysis (TGA)

Thermal gravimetric analysis (TGA) is a method of thermal analysis that provides to measure changes in physical and chemical properties of materials as a function of increasing temperature with constant heating rate. To determine the temperature range at which calcination of MCM-41 should be carried out TGA analysis used with constant heating rate [24].

1.6. Applications of MCM-41

Uniformly hexagonal array of linear channels and meso structure over long range make MCM-41 promising in many areas, such as shape selective catalysts or catalyst supports, host materials and in industry as adsorbents, ion exchangers and environment controller [42, 43].

MCM-41 type of materials can be used as shape selective catalysts as it demonstrates the ability to convert bulky molecules that are too large to react within the classical microporous molecular sieve pores [44]. If no catalytically active sites can be generated in the structure, properties of the MCM-41 are useful for producing carriers on which catalytically active phases such as heteropolyacids, amines, transition metal complex and oxides can be supported. Moreover, Bronsted acid sites can be generated on the surface of the MCM-41 mesopore structure. It is also possible to increase basicity of MCM-41 by exchanging the protons by alkaline ions and can be used base-catalyzed reactions. To give catalytic redox properties to MCM-41 transition metals can be introduced in the walls of MCM-41 structure. [14].

Another area MCM-41 have received attention is in the area of separation and adsorption. The uniform pore structure within the mesopore range and the high pore volume makes MCM-41 usable for separations that vary from the removal of organic and inorganic

contaminants in waste streams to chromatographic media. Early work demonstrated the extraordinary high sorption capacity of MCM-41 for hydrocarbons such as benzene [44]. Sorption of several adsorbates on MCM-41, e.g., nitrogen, argon, oxygen, water, cyclopentane, toluene, and carbon tetrachloride, and alcohols have been explored [5]. Researches about the adsorption capacity of MCM-41 showed that the modification of the pore walls by post functionalization change the sorption capacity and behavior of these materials. Replacing the surface silanol groups with trimethylsilyl groups creates more hydrophobic environment in the pore structure which reduces the sorption's capacity of polar molecules like water. In addition, uniform mesostructures MCM-41 synthesized as membranes used in separation applications of chemicals and pharmaceuticals [44]. Interestingly, MCM-41 offers a method for the recovery of some heavy metal ions such as mercury, lead, and silver from liquid pollutants. MCM-41 has shown a remarkable ability to sop up heavy metal ions from wastewater; therefore it can be used in environmental and industrial pollution control processes [5,44].

MCM-41 is considered as promising material for the loading and encapsulations of various metals, metal oxides, semiconductor cluster and nanowires due to its mesopore structure. Besides these applications of MCM-41 it has speculated that MCM-41 materials could show utility in a variety of electronic, optical and other advanced applications [44]. It has been demonstrated that 2,4,6-triphenylpyrylium (TP⁺) cation incorporated in MCM-41 can be used as a highly efficient electron-transfer material [45].

1.7. Adsorption on Porous Materials

Adsorption is the enrichment of one or more components in an interfacial layer which occurs when an adsorbable gas (the adsorptive) comes into contact with the surface of a solid (the adsorbent). The interfacial layer composed of two regions: the surface layer of the adsorbent and the adsorption space in which enrichment of the adsorptive can occur. The material in the adsorbed state is known as the adsorbate, as distinct from the adsorptive, i.e. the substance in the fluid phase which is capable of being adsorbed [46].

Adsorption is the process in which adsorptive molecules are transferred to, and accumulate in the interfacial layer. Desorption is the converse process of adsorption in which adsorbed amount decreases. Many adsorbents are porous materials with high surface areas. According to physisorption, porous materials are classified due to their pore sizes:

- macropores with pore diameter larger than 50 nm,
- mesopores with pore diameter between 2 nm and 50 nm,
- micropores with pore diameter not exceeding 2 nm.

Pore filling mechanisms depends on the pore shape, size and are affected by properties of the adsorptive and adsorbent–adsorbate interactions.

The relation between the amount adsorbed and the equilibrium pressure of the gas can be determined at constant temperature which is known as adsorption isotherm. According to IUPAC classification adsorption isotherm can be grouped into six types. These types are shown in Figure 1.10. [46].

Microporous adsorbents which are having relatively small external surfaces give Type I isotherms. Activated carbons, many zeolites and certain porous oxides are some examples of the adsorbents that gives isotherms of Type I.

Reversible Type II isotherm is the normal form of isotherm obtained with a non-porous or macroporous adsorbent. The Type II isotherm represents unrestricted monolayer-multilayer adsorption. Point B, the beginning of the almost linear middle section of the isotherm, is

often taken to indicate the stage at which monolayer adsorption is complete and multilayer adsorption about to begin.

In addition to Type II isotherm Type III isotherms describe adsorption on macroporous materials. Macroporous materials with strong adsorbent-adsorbate interactions display Type II isotherm. On the other hand, macroporous materials with weak adsorbate-adsorbent interactions display Type III isotherm [47].

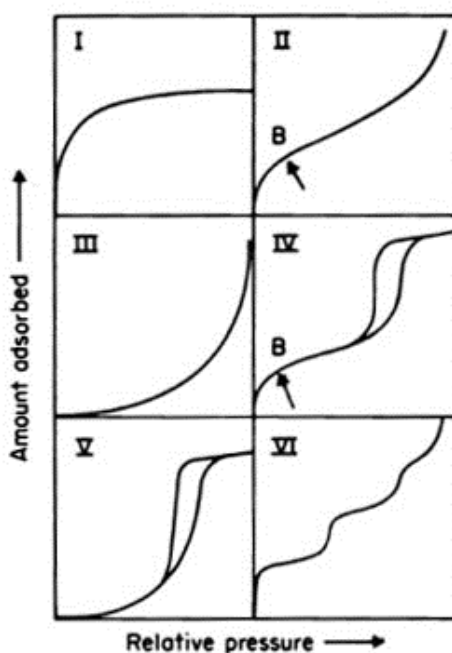


Figure 1.10: IUPAC classification types of adsorption isotherms [46]

Type IV adsorption isotherm is given by mesoporous materials. Also Type V isotherms characterize mesoporous adsorbents with weak interactions between adsorbate-adsorbent, whereas Type IV for strong adsorbate-adsorbent interactions [46,47].

The sharpness of the steps of Type VI isotherm depends on the system and the temperature and this type of isotherm represents stepwise multilayer adsorption on a uniform non-porous surface. Best examples of Type VI are argon or krypton sorption on graphitized carbon blacks at liquid nitrogen temperature [46].

Adsorption hysteresis is observed when the adsorption and desorption curves do not coincide. For lower temperatures Type IV and Type V isotherms show hysteresis loops which are associated with capillary condensation taking place in mesopores, and the limiting uptake over a range of high p/p_0 . Types of hysteresis loops are shown in Figure 1.11 [46]

It is hard to understand factors affecting the adsorption hysteresis but for some mesoporous adsorbents the shape of the hysteresis loop gives a identification of the type of pore structure in the respect of uniformity and shape of the pores [46, 48]. Therefore, H1 type of hysteresis which is a fairly narrow related with capillary condensation in open-ended cylindrical pores [49].

Many porous adsorbents like inorganic oxide gels and porous glasses tend to give Type H2 loops. In this type pore size and shape are not well defined. From the H2 type of hysteresis

loops interpretation, spheroidal cavities or voids as well as ink-bottle pores are recognized, however this explanation of H2 loops is oversimplified. The pore characters of materials which have these loops, have more complex pore structures with interconnected networks. Until relative pressure is decreased to allow evaporation from the neck, the liquid seems to be trapped in the body of the pore; therefore, the release of condensate is limited by the dimension of the neck radius [46,49].

H3 loops do not indicate a limiting adsorption at high p/p_0 and these loops are given by aggregates of plate-like particles or adsorbents containing slit-shaped pores. In addition, Type H4 is related with slit-shaped pores but in the case of microporous materials [46].

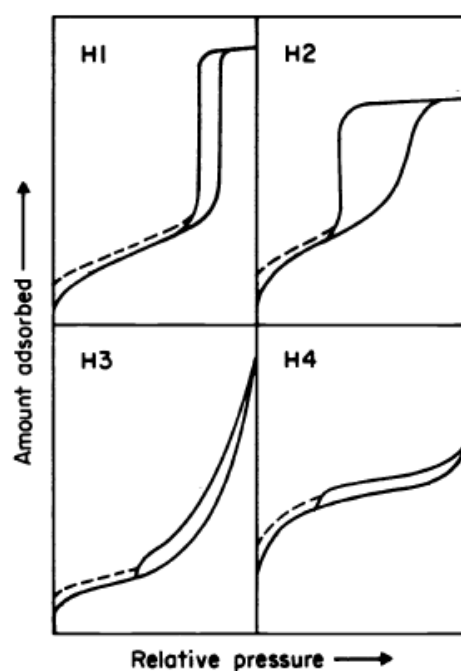


Figure 1.11: Types of hysteresis loops

1.8. Aim of This Study

The aim of this study is to determine the sorption capacities of p-xylene, m-xylene, o-xylene and ethylbenzene on MCM-41 type of mesoporous material with high surface area which was synthesized in this study with CTAMBr (as surfactant) and TEOS (as silica source). Moreover to compare these sorption capacities with the sorption capacities on different MCM-41 sample with low surface area and pore volume that was used in a previous study and to observe the effect of the adsorbent's properties on the sorption capacities of o-, m-, p-xylene and ethylbenzene on MCM-41. For this purpose by using IGA system which is an automated gravimetric electro balance system, at different temperatures that are 30°C, 50°C and 65 °C isotherm data was obtained.

CHAPTER 2

LITERATURE SURVEY

Molecular sieves with a structure and pore diameter of zeolites select shapes which makes them good adsorbents or catalysts. However, channel diameters at mesopore region are necessary for reactions with bulky molecules [3]. Therefore, researchers tried to synthesize large pore frameworks by combining the concepts of pillared layered materials and the formation of zeolites. During these studies, MCM-22 was discovered [18]. MCM-22 zeolite was composed of crystalline layers that were linked together by weak chemical bonds during the synthesis. Upon thermal treatment, these chemical linkages became much stronger, as the layers condensed onto each other. By the delaminating or separation of crystalline layers of the MCM-22 “precursors” before any thermal treatment, a pillared layered material obtained called MCM-36. In the initial layers of intercalation process an alkyltrimethylammonium compound was used and stable inorganic pillars were inserted with a reactive silica source such as tetraethyl ortosilicate. As a result of interrupting the synthesis of zeolite and using these crystalline layered materials as reagents to form large pores by isolating the zeolite precursors ZSM-35 zeolite family was determined. The zeolite synthesis was interrupted before any X-ray diffraction evidence of crystallinity. To this interrupted zeolite precursor media high concentrations of an alkyltrimethylammonium salt at high pH were added and a reactive silica source, tetramethylammonium silicate, was also added as a potential pillaring agent. These new synthesis mixtures were subjected to additional hydrothermal treatment. The resulting product was a new family of molecular sieve called M41S family which differs from the zeolites with only one broad low-angle X-ray diffraction peak and the uniquely high values for both surface area and hydrocarbon sorption [21].

M41S family materials have unique physical and chemical properties. These ordered mesoporous materials generally, have large surface area, above 1000 m²/g and pore diameters are between 2- 50 nm. Also these materials surfaces have active centers. Therefore their surfaces can be decorated or modified easily [22]. In this family three different mesophases have been identified which are, MCM-41 with hexagonally-ordered pore structure, 3-D MCM-48 with cubic-ordered pore structure and MCM-50 with unstable lamellar structure [21]. Among M41S family MCM-41 has attracted more attention of scientist due to its high surface area, high thermal and hydrothermal stability, controllable pore size, hydrophobicity and acidity. This porous material composed of hexagonally arranged channels with pore diameters varying from 1.5 to 10 nm. These features of this material make it a promising material as catalyst and support and can be usable in the industry for adsorption, ion exchange and environmental control [3].

About seventy years ago physical adsorption of nitrogen at 77 K were undertaken by Brunauer and Emmett. Then to determine surface area and pore size distribution of a wide range of porous materials low temperature nitrogen adsorption was accepted as standard procedure. In 1938 BET theory by Brunauer, Emmett and Teller was published for nitrogen adsorption. The most widely used procedure for the pore size distribution from nitrogen adsorption data is based on the principles developed by Barrett, Joyner and Halenda. To characterize a porous solid, physisorption are carried out at constant temperature and adsorption isotherm data observed. This isotherm shape features give information about the gas-solid interaction, surface area and the porosity of the adsorbent [41]. The classification

of pores according to their size and the relation between the amount adsorbed and the equilibrium pressure of the gas according to IUPAC explained under the Adsorption on Porous Materials heading.

In the study of Branton et al., MCM-41 was characterized by investigation of adsorption of several molecules [6]. The adsorption isotherm of argon, nitrogen, and oxygen on MCM-41 sample with the surface area $655 \text{ m}^2/\text{g}$ and pore diameter in the range 3.3-4.3 nm were determined. In this study all isotherms were type IV according to the IUPAC classification. The argon and oxygen isotherms exhibit well defined hysteresis loops which is generally found with well defined mesoporous adsorbents. On the other hand, the nitrogen isotherm was completely reversible. They concluded that the absence of hysteresis is because of the particular pore shape and size distribution, which results in capillary condensation /evaporation taking place reversibly in the region over $P/P_0 = 0.42$ [50].

To understand the effect of pore size on the adsorption nitrogen adsorption isotherms have been measured on a series of aluminosilicate and titanosilicate MCM-41 molecular sieves. These MCM-41 samples had mean pore radius varying from 0.9 to 2 nm. By comparing plots it is concluded that the nature of the adsorption on these materials depend strongly on their pore size. If pores of radius are around 1 nm multi layer coverage of the pore walls occurs. If the radius is increased to 1.5-1.8 nm the mechanism of adsorption changes into a two-stage process. The multilayer coverage of the pore walls is succeeded by the spontaneous filling of the pore volume by capillary condensation without hysteresis. For the larger pores the usual capillary condensation with hysteresis occurs [51].

The adsorption isotherms of methanol, ethanol, propan-1-ol, butan-1-ol, and water vapor on MCM-41 sample at different temperatures which are 290K, 298K, and 303K were studied. Adsorption isotherms of alcohols are all type IV according to IUPAC classification. On the other hand the water isotherm is type V. Each adsorption isotherm exhibits a sharp step, indicative of capillary condensation within narrow distribution of mesopores. The isotherms are reversible in the monolayer-multilayer region; however distinctive hysteresis loops are related to the condensation- evaporation cycle. The area within the loop depends on the adsorbate. The area within the loop increased in scale from methanol to butan-1-ol and water. This study showed the large internal surface of MCM-41 is somewhat hydrophobic and that its mesopore structure is remarkably uniform and stable [52].

Adsorption characterization of MCM-41 by using benzene adsorption isotherms studied on three MCM-41 samples. These three MCM-41 samples synthesized with TEOS as silica source and octyltrimethylammonium (C8), decyltrimethylammonium (C10) and cetyltrimethylammonium (C16) bromides as templates. These samples were exposed to relatively long thermal treatment which provides well ordered pores observed by XRD characterization. Benzene adsorption isotherms measured on these MCM-41 samples were used to evaluate the BET specific surface area, total pore volume, external surface area, the volume of ordered mesopores, and to obtain the statistical film thickness as well as the Kelvin-type relation, which describes the dependence between pore width and condensation pressure for benzene on silica at 298K. [53] Besides it was reported that the pore volumes evaluated from benzene, neopentane, n-hexane and methanol adsorption data for the MCM-41 studied were comparable but smaller than the corresponding pore volumes obtained from nitrogen adsorption [54].

Nitrobenzene adsorption from aqueous solution on MCM-41 was investigated by using batch experiments. Nitrobenzene adsorption is initially rapid and the adsorption process reaches a steady state after 1 min. The effect of temperature, pH, ionic strength, humic acid, and the presence of solvent on adsorption processes were examined. The observation shows that, the amount of nitrobenzene adsorbed decreases with an increase of temperature, pH, and ionic strength. However, the amount of nitrobenzene adsorbed onto MCM-41 was not affected significantly from the presence of humic acid. Organic solvent causes a decrease in nitrobenzene adsorption [55].

To determine the effect of temperature on the adsorption isotherms and on the capillary condensation/evaporation processes of toluene, methylcyclohexane, and neopentane on MCM-41 material, adsorption of toluene, methylcyclohexane, and neopentane on silica MCM-41 studied. The adsorption isotherms of toluene and neopentane were found to be type IV according to IUPAC classification which is similar to adsorption type of nitrogen on MCM-41. However adsorption isotherm methylcyclohexane did not show a knee at low P/P₀, meaning weak adsorbate-adsorbent interactions. Moreover it was observed that neopentane adsorbs reversibly in the range of temperatures studied. On the other hand, at the lowest temperatures the isotherms of toluene and methylcyclohexane exhibited a hysteresis cycle. These two organic adsorbents have very close hysteresis critical temperatures, whereas the stepwise capillary condensation occurs at different P/P₀. This study showed that the three organic adsorptives interact differently with silica surface and the isosteric heats of adsorption indicated that methylcyclohexane has the weakest interaction and toluene the strongest [56].

The effect of cationic template on the adsorption of aromatic compounds on MCM-41 was investigated by measuring adsorption equilibrium of toluene, cumene and water on MCM-41 with digital microbalance. By controlling the template removal in the synthesis procedure in which cationic surfactant used as template different MCM-41 samples were prepared. The synthesized samples were characterized with X-ray diffraction (XRD), nitrogen adsorption, FTIR and TGA. When MCM-41 which is a synthesized by removing template completely compared with C-MCM-41 which is synthesized by removing template partially, C-MCM-41 exhibited moderate adsorption capacity for aromatic compounds. On the other hand, the adsorption equilibrium of water showed that the hydrophobicity on the surface of was significantly enhanced. For the VOCs removal process the combination of moderate adsorption capacity for aromatics and hydrophobicity for water is a desired feature. Porosity and cationic spots generated by cationic templates affect the adsorption behaviors of aromatic compounds and water on various MCM-41 samples. The porosity and cation density of the MCM-41 material can be adjusted by controlling the removal of the cationic template from the pore structure [57].

The effect of surfactant template in MCM-41 and calcination on the phenol and o-chlorophenol removal was studied by adsorption of phenol and o-chlorophenol on a mesoporous MCM-41 material. In this study uncalcined MCM-41 shows significant adsorption for phenol and o-chlorophenol as compared to calcined MCM-41. This interesting result observed due to the hydrophobicity created by surfactant template in the MCM-41. To observe the effect of adsorbent dose, pH, initial concentration and the presence of co-existing ions, batch adsorption studies were carried out. As a result of this studies it was seen that adsorption of phenol and o-chlorophenol depends on the solution pH and co-existing ions present in the aqueous solution. The uptake of o-chlorophenol was higher than phenol on MCM-41 [58].

The potential of MCM-41 to remove dyes from aqueous solution was examined with adsorption of organic dye (methylene blue) on MCM-41. To understand adsorption characteristic of MCM-41, adsorption of methylene blue on MCM-41 was measured with respect to contact time, pH and temperature. Both Langmuir and Freundlich adsorption models were applied to describe the equilibrium isotherms. MCM-41 sample used in this study was characterized by nitrogen adsorption/desorption isotherms, XRD and TGA [59].

To determine simple and effective adsorbents to eliminate anionic surfactants from water the partial removal of the structure directing templates from MCM-41 was studied. Cetyltrimethylammonium (CTMA) used as template were removed from the as-synthesized MCM-41 samples by ion-exchange in alcoholic ammonium nitrate solutions. Standard characterization techniques were used to characterize the treated samples. The surface structure and distribution of CTMA species in the modified samples were altered by ion exchange. The new formed hydrophobic species used for adsorption of sodium dodecyl

sulfate (SDS). Formations of CTMA⁺ bilayers in these samples provide suitable conditions for hydrophobicity and electrostatic interactions between SDS and CTMA. As a result these samples were loaded by SDS remarkably. The products with low-content of CTMA or without CTMA were very poor adsorbents. The maximum SDS adsorption capacity observed with superior sample is 646.6 mg/g [60].

Adsorption isotherms of aromatic hydrocarbons such as benzene, toluene, p-xylene, and mesitylene on high-silica MCM-41 (Si-MCM-41) at different temperatures (348-498 K) was studied by gas chromatographic technique. The isosteric heats of adsorption of the aromatic hydrocarbons at different loadings were determined from the adsorption isotherms. According to results it was found that isosteric heats of hydrocarbons ordered as Q_a (benzene) < Q_a (toluene) < Q_a (p-xylene) < Q_a (mesitylene). As adsorbate loading increased, the heat of adsorption of all the aromatic hydrocarbons decreased. At intermediate adsorbate loading the decrease for the benzene adsorption was remarkable. This decrease indicated surface heterogeneity because of the presence of adsorbed benzene. Entropy analysis of the adsorption indicated that the adsorbed aromatic hydrocarbons except benzene are neither completely mobile nor localized. Only the benzene is completely mobile or even super mobile. When adsorbate loading increased the mobility of the adsorbed toluene, p-xylene, and mesitylene is decreased [61].

Sorption of C₈ aromatics on MCM-41 was studied with m-xylene, p-xylene, o-xylene and ethylbenzene at different temperatures (30 °C, 50 °C, 65 °C and 80 °C) by using gravimetric system. Used MCM-41 sample with average pore diameter had relatively low surface area which was 492.2 m²/g. The used MCM-41 sample was synthesized by hydrothermal synthesis method in basic conditions by using CTAMBr as surfactant and sodium silicate as silica source. In synthesis of MCM-41 pH was adjusted to 11 by using H₂SO₄. In this study, the amounts of each sorbate (p-xylene, m-xylene, o-xylene, and ethylbenzene) adsorbed at a given relative pressure on MCM-41 decreased when the temperature of the adsorption isotherms increased. All adsorption isotherms demonstrated type V of isotherm, according to IUPAC classification due to the mesoporous nature of the MCM-41 sample. As the temperature for the adsorption isotherms increased the size of hysteresis decreased for each sorbate which is associated with condensation-evaporation within a narrow distribution of mesopores. The volumes of sorbates (V_p) were obtained from the mass uptake at maximum relative pressure with normal liquid density at the adsorption temperature for all sorbates. These volumes of sorbates were significantly lower than the volume obtained from low-temperature nitrogen isotherm because the density of the adsorbed phase was not same as that of the liquid adsorptive. Curvature of some isotherms at high relative pressure also leads to uncertainty in the location of the upper limit for pore filling [62].

CHAPTER 3

EXPERIMENTAL

In this study, first adsorbent MCM-41 was synthesized. Then adsorption isotherms of p-xylene, m-xylene, o-xylene on the synthesized MCM-41 investigated by IGA (Intelligent Gravimetric Analyzer) system at different temperatures that are 30 °C, 50 °C and 65 °C. In addition to xylenes, ethylbenzene adsorption isotherm data was obtained at 30 °C, 50 °C and 65 °C.

3.1. MCM-41 Synthesis Procedure

MCM-41 sample used in this study was synthesized according to hydrothermal synthesis route procedure as described in a previous study [19]. For the MCM-41 synthesis a silica source, surfactant and solvent are needed. CTMABr (cetyltrimethylammoniumbromide) used as surface-directing surfactant, water was used as solvent and TEOS (tetraethylortosilicate) used as silica source [19].

For the synthesise of MCM-41, first 13.2 g CTAMBr dissolved in approximately 87 ml deionized water and continuously stirred at a rate of 500 rpm at 30 °C. Temperature of the solution was kept at same temperature to avoid formation of agglomerates due to temperature change. After clear solution was observed 15.6 ml TEOS was added drop wise while stirring. After addition of TEOS pH of the solution was stabilized at 4.2. Then pH of the solution was adjusted to 11 with addition of 1 M sodium hydroxide (NaOH) and kept stirred for an hour. Finally solution was transferred to a teflon bottle and placed in a stainless-steel autoclave. The hydrothermal synthesis was carried out at 120 °C for 96 h. Resultant solid was filtered and washed with deionized water to remove excess template and ions that did not enter the formation of the structure. While washing the solid it was too concentrated and did not allow water to expose to the pores. To overcome this situation, material was taken into a beaker, suspended in water and stirred for 15 minutes. This step was repeated until the pH of the residual water remained constant at 8.6. Finally the product was dried at room temperature and calcined in a tubular furnace at 540 °C for 8 h with a flow of dry air to remove organic materials within the pores. Synthesis steps for MCM-41 material can be seen in Figure 3.1.

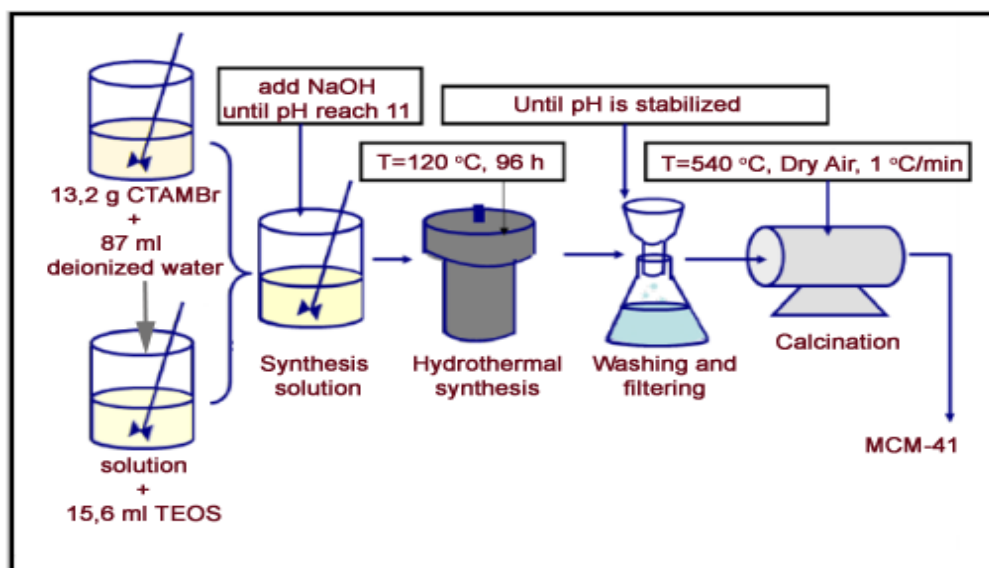


Figure 3.1: Synthesis steps of MCM-41 [Adapted from 19]

3.2. Investigation of Adsorption Isotherms

The adsorption isotherms of p-xylene, m-xylene, o-xylene and ethylbenzene on MCM-41 were investigated by IGA system. These isotherms were determined at different temperatures 30°C, 50°C and 65°C for p-xylene, m-xylene and o-xylene. Ethylbenzene adsorption data on MCM-41 was obtained at 50°C.

3.2.1. Intelligent Gravimetric Analyzer (IGA)

The model IGA-002- vapor sorption system is specifically designed to study water and vapor sorption. The system is available in a high vacuum configuration which enables porous materials to be studied. The model of IGA-002 contains the following parts:

- computer-controlled microbalance system,
- stainless steel vacuum-pressure vessel to ultra high vacuum standards,
- two low and high pressure sensors (100 mbar and 10 bar)
- stainless steel reactor,
- adsorbate reservoir,
- cabinet door for access to an internal port for the connection of the adsorbate reservoir,
- manual isolation valve and a purge valve for the adsorbate reservoir,
- standard furnace,
- additional thermal insulation and heating system for the IGA cabinet,
- anti-condensation system (max 50 °C),
- software upgrade incorporating interactive vapor pressure calculator based on Antoine coefficients.

The IGA system is shown in Figure 3.2 and also IGA-002 configuration which is used in the experiment in this study is shown schematically in Figure 3.3.



Figure 3.2: IGA system

The IGA makes gravimetric analysis with microbalance system it contains. This microbalance part contains the pan that MCM-41 sample put in. The computer-controlled system IGA provides fully automatic and reproducible determination of adsorption isotherms by measuring weight, pressure and temperature change. Two levels of vacuum offered to vacuum systems for de-pressurization and outgassing. Rotary pump can be used for operation to 10^{-2} mbar, on the other hand a turbo molecular pump can be used for operation to 10^{-6} mbar. The system have two pressure sensors and selection of pressure sensors enables pressure control at very low partial vapor pressures. Standard furnace can be used up to 500°C. For the isotherm measurements furnace temperature set-point regulation is between 20°C-500°C. The protection against condensation is done by 'Anti-condensation protection part' and this part operates in conjunctions with thermostats and temperature sensors to define and measure the temperature of the chamber.

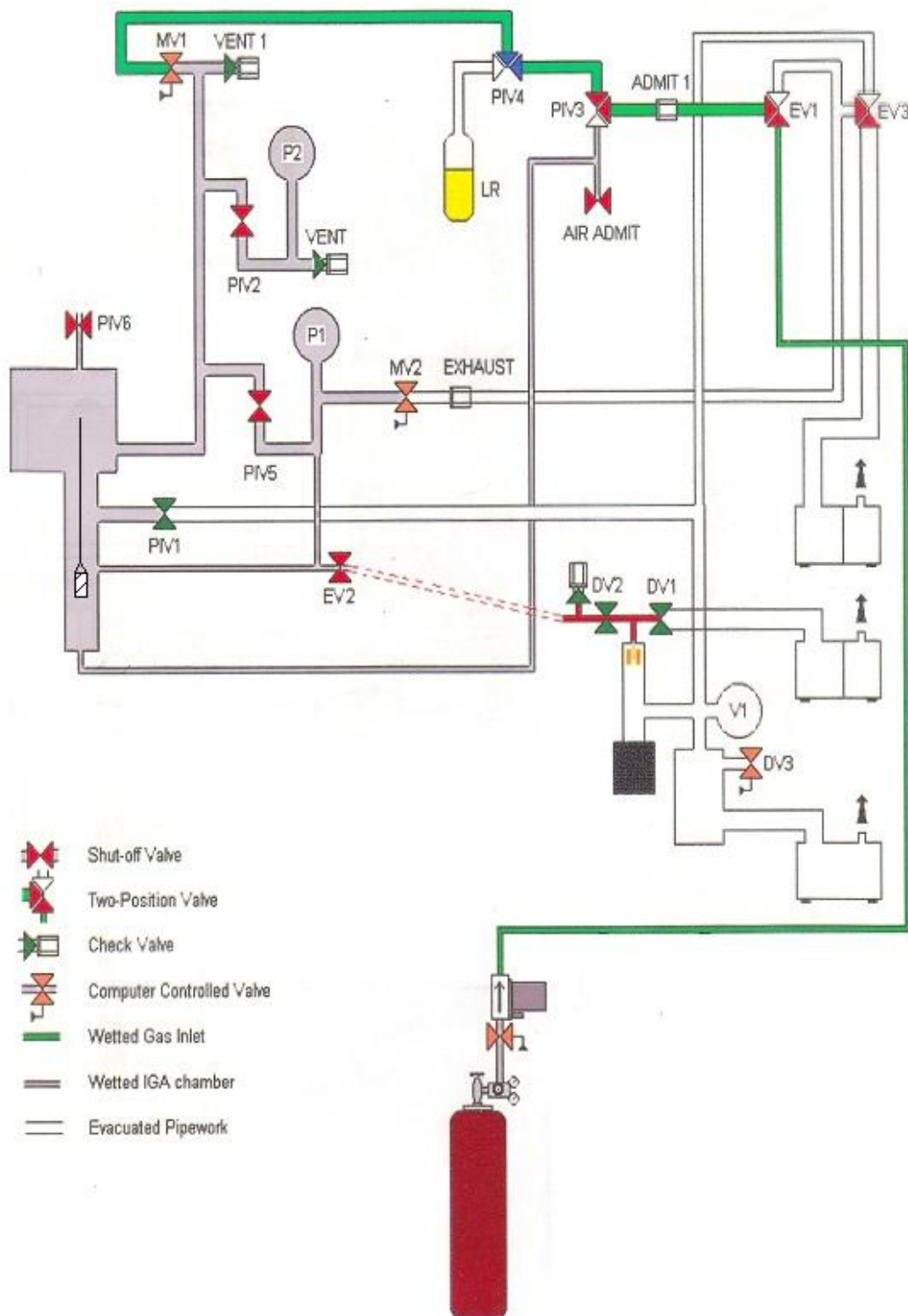


Figure 3.3: IGA-002 configuration set for vapor sorption operation (Idle mode)

3.2.2. Experimental Procedure

The steps to determine adsorption isotherms of p-xylene, m-xylene, o-xylene and ethylbenzene on MCM-41 by using an automated gravimetric electro balance system IGA (IGA-002 configuration, HIDEN) is shown in Figure 3.4. In addition detailed information about the IGA system can be seen in Appendix D.

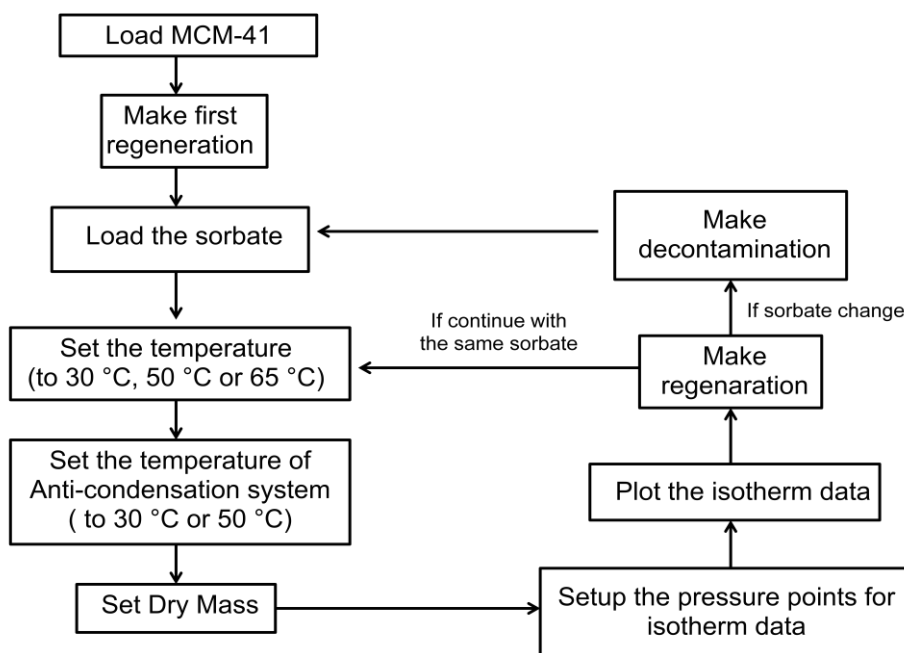


Figure 3.4: Experimental procedure steps of adsorption isotherm data

3.2.2.1. Loading MCM-41 Sample

To load a new sample first the old sample should be unloaded. For the unloading and loading procedures IGA software guides us. To start to unloading procedure pressure and temperature control should be stopped and then we let the air enter to the reactor before starting the unload procedure of the sample. Lower the sample reactor while supporting the reactor tube as shown in Figure 3.5. To ensure that the reactor is kept upright while lowering until it is clear of the sample position [63].

The sample container (pan) should be removed by using the container carrier. Then remove the old pan and attach the new pan that contains MCM-41 sample, again by using pan carrier. Same pan can be used for the new sample or can be replaced with a new pan. If same pan is used, the meter reading and the loading values appear similar to displayed before. If the pan changed weight of the new pan should be recorded and new load of the sample is adjusted according to this record. Loading the pan can be seen in Figure 3.6. After loading the pan with the sample the reactor tube should be replaced and tightened.

Each new sample is given an identification sample number between 2 and 9999. The sample number is ultimately displayed at the top of the screen together with a title. The combination of number and title are used to identify the experiments.



Figure 3.5: Lowering the sample reactor [63]



Figure 3.6: Loading sample container (pan) [63]

3.2.2.2. Regeneration

After the sample MCM-41 is loaded regeneration of sample is carried out. In addition, after every sorption experiment, regeneration of MCM-41 sample is needed to use the same sample. Regeneration starts by selection “Outgas” (vacuum drying) from the pressure control window for degassing the reactor. Outgas ramp rate was 10 mbar/min which is recommended for the powder samples. If regeneration started after experiment the PIV4 valve should be rotated to vertical position (close position) to isolate sorbate reservoir. For de-pressurization computer controlled valve MV-2 is fully opened to the vacuum pump and entire chamber is evacuated. After MV-2 valve is fully opened chamber is connected to turbo molecular pump by rotating the EV-4 valve (seen in Figure 3.7) to upward. EV-4 valve provides connection to rotary (to downward) or turbo molecular pump (to upward). The high conductance exhaust valve PIV-1 was also gently opened at this stage to improve the efficiency of evacuation and the control PIV1 must be selected in the pressure set window. Then MCM-41 sample is heated up to 200°C with ramp rate (5°C/min) under high vacuum (10^{-6} mbars) for four hours. After four hours of evacuation zero point of pressure sensor is reset using the Zero function on the pressure set window. Then, PIV-1 valve and the vacuum valve EV-4 are closed (horizontal position). Then MCM-41 sample is set to the next isotherm experiment temperature by setting the temperature on the temperature set window.

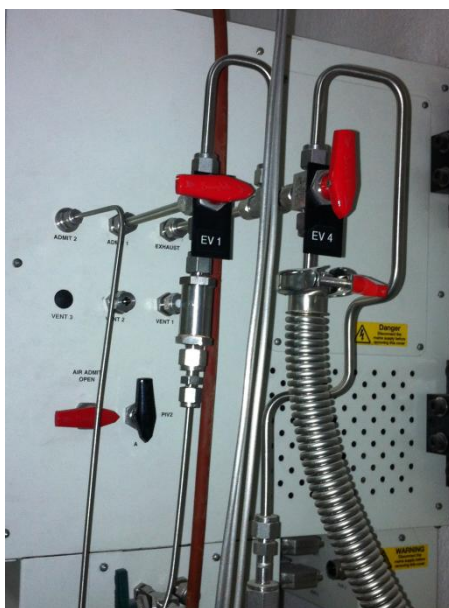


Figure 3.7: Manual vacuum valve

3.2.2.3. Loading the Sorbate

To load the sorbate first front access cover of the IGA should be removed. PIV-4 valve should be in vertical position which means reservoir is isolated. The stainless steel liquid reservoir which shown in Figure 3.8 is removed by loosening off the VCR holding nut with “ $\frac{3}{4}$ ” spanner. The removed reservoir can be emptied, cleaned and baked out or replaced with an alternate reservoir. In this study same reservoir was used. If the sorbate is to be changed, empty reservoir should be moved back into position and retightened and the vapor delivery pipe work should be decontaminated. On the other hand, if continues with the same sorbate there is no need to decontamination. For both case, after reservoir is filled with the sorbate it is reattached into its position. To remove air in the reservoir, while EV-4 connected to rotary pump EV-1 (seen in Figure 3.7) is rotated to upward to vacuum the line up to PIV-4 valve. Then PIV-4 is rotated to left and right slowly and repeated about ten or more times. By the way air in the reservoir is evacuated.

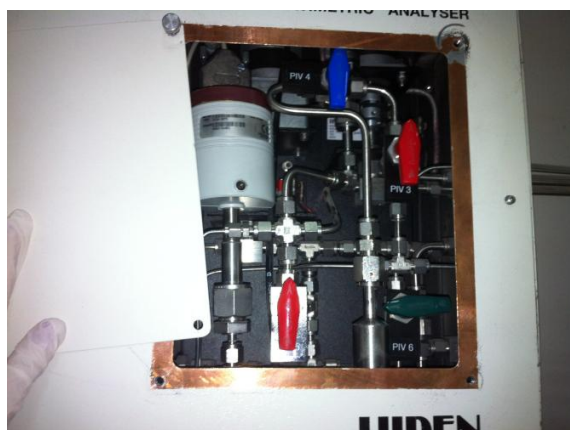


Figure 3.8: Liquid reservoir

3.2.2.3.1. Sorbates

P-xylene, m-xylene, o-xylene and ethylbenzene are the sorbates used in this study. The sorbates were used without any purification step and their grades and sources are given in Table 3.1.

Table 3.1: Grades and origins of sorbates

Sorbate	Grade	Supplier
p-xylene	Chemically pure	Fluka
m-xylene	Chemically pure	Fluka
o-xylene	Chemically pure	Fluka
Ethylbenzene	Chemically pure	Fluka

Vapor pressure calculator in the IGA system is based on Antoine equation. Antoine coefficients, critical temperatures and vapor pressures of sorbates at 30°C, 50°C, 65°C are given in Appendix A. After the sorbates are loaded, from the vapor pressure calculator vapor pressure for the temperature at which adsorption isotherm data will be determined, is calculated. When setting up the isotherm pressure points system calculates the relative pressures and do not let pressure points exceed the vapor pressure at that temperature to prevent condensation.

3.2.2.3.2. Decontamination

Decontamination provides removing impurities from the gas or vapor connection lines of the system. When sorbate is changed decontamination is a necessary process. Before starting the decontamination pressure control should be inactive. Also it is necessary to ensure that PIV 1 valve at the bottom (green valve) of the IGA is closed. First empty reservoir should be connected, and then PIV-4 should be rotated to left to connect the reservoir. From the pressure set window “Decontamination” is selected. System asks the current password to start the decontamination. When decontamination is started system opens the admittance valve (MV-1) fully. Then degas the reactor by selecting ‘Outgas’, from pressure control window with a ramp rate 10 mbar/min. As the admit valve is fully open, the vapor admit pipe work will be decontaminated as the entire system is evacuated. After the PIV-1 button in pressure set window become active PIV1 button from pressure set window is selected and slowly opened. With the “Stop” in the pressure set window decontamination can be finished.

3.2.2.4. Setup the Temperature of Isotherm

The temperature control parameters and options are set or changed in the temperature set window which is shown in Figure 3.9

Temperature which is the furnace temperature was set to 30 °C, 50 °C and 65 °C for the adsorption isotherms in this study. Ramp rate was 5 °C/min as recommended.

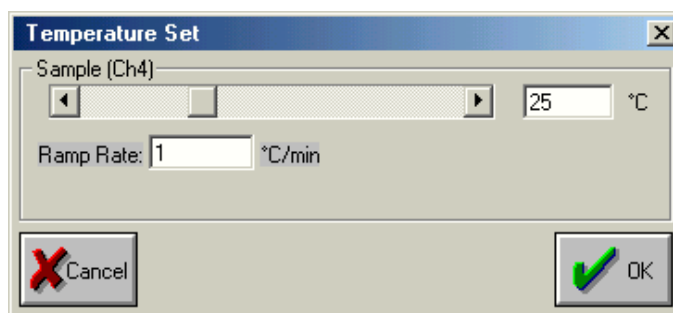


Figure 3.9: Temperature setup window

3.2.2.5. Setup the Temperature of Anti-condensation System

The temperature of “Anti-condensation system (ACS)” was set up according to isotherms temperatures to avoid the condensation in the chamber. “ACS temperature” was specified as 30 °C when the adsorption isotherm temperature was 30 °C. When adsorption isotherm temperature was 50 °C and 65 °C “ACS temperature” was set to 50 °C for both because the maximum temperature that can be set is 50 °C.

3.2.2.6. Setup the Pressure Points for Adsorption Isotherm

The sorption/desorption pressure points are entered from the isotherms setup window which can be seen in Figure 3.10.

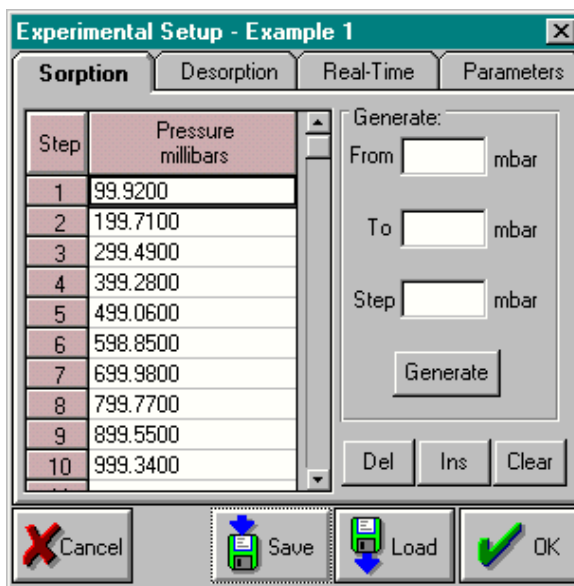


Figure 3.10: Isotherm setup window

The sorption set-points must be increasing pressure values in the grid order according to the saturated vapor pressure of the sorbate at the isotherm temperature, desorption set-points must be decreasing pressure values in the grid order, blanks are not allowed and the pressure change must be at or above the minimum control increment (equivalent to ~ 0.05%)

of the pressure range). In addition, during the experiment, the pressure values may not exactly correspond with the grid. The reason is that, for example, on adsorption the software checks the grid for the next highest pressure above the minimum control increment. This means that we can start the isotherm with any initial pressure in the chamber and on adsorption the first isotherm point will be the next highest grid value for which the pressure change is above the minimum increment.

3.2.2.7. Plot Isotherm Data

Equilibrium data (for selected x, y1-or y2- axis fields) were plotted by the selection of, Replay Isotherm tool, from tool Bar in the IGA software window. The sample run number is selected from drop-down file select list at the top of the window and then the required isotherm scans were selected too in the plot column and then the graph produced. The isotherm is typically plotted as x-field = P/P_0 and y-field= % mass.

CHAPTER 4

RESULTS AND DISCUSSION

In this chapter, the characterization results of MCM-41 sample that was synthesized in this study by XRD, nitrogen physisorption analysis, TEM, SEM, EDX and TGA are and the sorption capacities of p-xylene, m-xylene, o-xylene, and ethylbenzene on MCM-41 are presented. Detailed data can be found in Appendix B.

The adsorption isotherms of p-xylene, m-xylene and o-xylene on synthesized MCM-41 were measured at different temperatures 30°C, 50°C, 65°C. In addition, to see the ethylbenzene sorption capacity on MCM-41 its adsorption isotherm was determined at same temperatures of xylene adsorption isotherms. During the sorption experiments, initial pressure was around 10^{-7} milibars and final pressures changed according to the vapor pressure of the sorbates at isotherm temperatures. However, final vapor pressures of isotherms that are determined at 65 °C were setup according to vapor pressure of the sorbent at 50 °C, because the maximum temperature of 'Anti-condensation system' part in IGA system is 50 °C and to the prevent condensation in this chamber pressure of sorbate should be kept below the vapor pressures of adsorbates at 50°C. Vapor pressure calculator in the IGA system based on Antoine equation, therefore the Antoine equation and their constants are given in Appendix A.

4.1. Characterization of MCM-41

MCM-41 sample was synthesized by using the CTAMBr (as surfactant) and TEOS (as silica source) and this sample characterized by XRD, nitrogen physisorption analysis, TGA, TEM and SEM. Also EDX analysis was performed.

4.1.1. X-Ray Diffraction (XRD) Analysis

XRD provides direct information of the crystal structure of the materials. The XRD analysis of MCM-41 sample was performed by Rigaku Ultima IV X-ray Diffractometer in Central Laboratory, METU and is given in Figure 4.1. It is seen that main characteristic peak for synthesized MCM-41 obtained at $2\theta = 2.285^\circ$. Three reflection peaks can be seen approximately at $2\theta = 2.59, 4.27^\circ$ and 4.5° .

It is reported that the XRD peaks of MCM-41 do not result from crystal structure in the atomic range, but from the ordered channel walls. [24] Since these materials are not crystalline at atomic level, no reflections at higher angles are observed. The XRD pattern of MCM-41 shows typically three to five reflections between $2\theta = 2^\circ$ and 5° , although samples with more reflections have also been reported [10]. MCM-41 sample XRD pattern gives a sharp (100) plane diffraction peak and three reflection peaks corresponding to (110), (200) and (210), which meant that the sample had an ordered pore structure [64].

MCM-41 which was synthesized in a previous study with the same synthesis method and the same surfactant and silica source showed a sharp peak at $2\theta = 2.6^\circ$ and three reflection peak values at approximately $2\theta = 3.02^\circ$ and 4.65° and 4.82° [19].

Sharp peak and the small reflection peaks observed from the XRD pattern of the MCM-41, which was synthesized and used as adsorbent in this study, indicated that the desired structure of MCM-41 was successfully synthesized.

Reflection angles corresponds the interplanar spacing values (d-spacing). From the d_{100} value which is obtained from the main peak, distance between the pore centers (a) can be calculated with the equation 4.1. Pore wall thickness is the difference between the a and the pore diameter as stated in the equation 4.2 [73]

$$a = 2 \times d_{100} / \sqrt{3} \quad (4.1)$$

$$b_d = a - w_d \quad (4.2)$$

Obtained d_{100} , a and b_d values are 6.428 nm, 7.422 nm and 4.67 nm respectively. Pore diameter was obtained from nitrogen adsorption analysis as 2.75 nm.

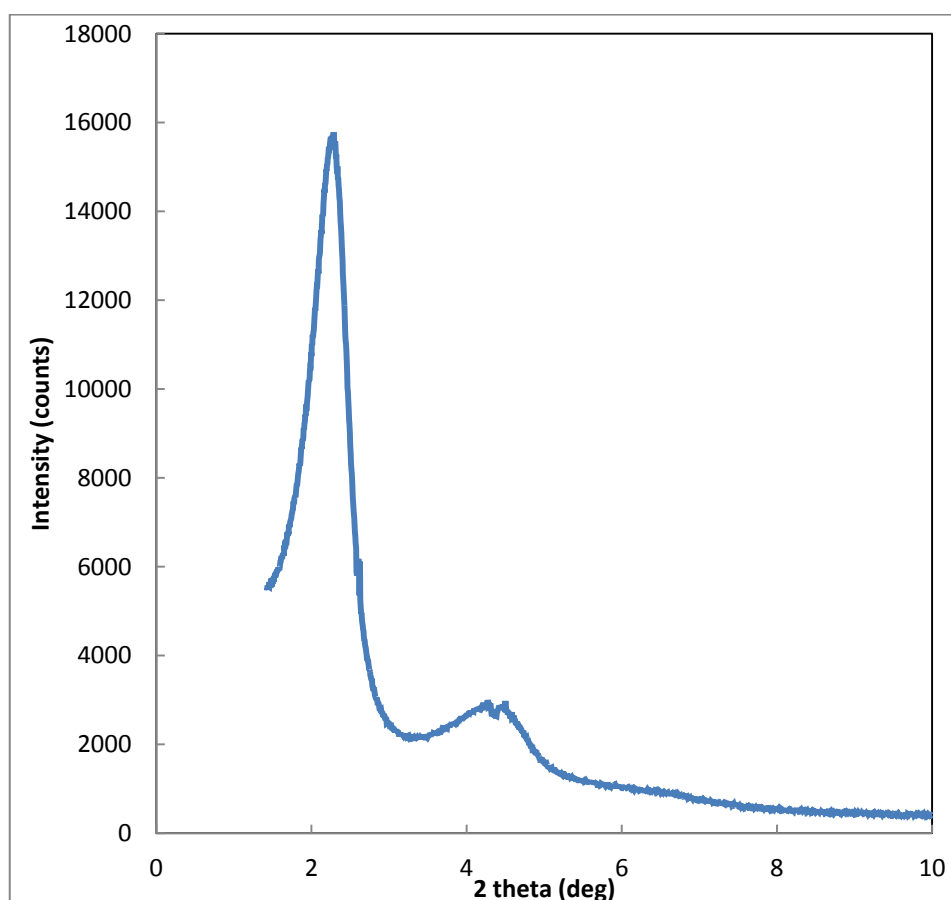


Figure 4.1: XRD pattern of MCM-41

4.1.2. Nitrogen Physisorption Analysis

From the nitrogen adsorption and desorption isotherms of MCM-41 at 77 K the BET surface area, the BJH desorption pore diameter and the multi point total pore volume of the synthesized MCM-41 sample were determined. Nitrogen adsorption experiments of MCM-41

sample were performed by Quantachrome Autosorb, Automated Gas Sorption System in Central Laboratory of Middle East Technical University.

The nitrogen adsorption isotherms of the calcined MCM-41 which is showed in Figure 4.2 showed a typical type IV isotherm according to IUPAC classification with strong interaction between the adsorbate-adsorbent. Nitrogen physisorption of MCM-41 demonstrates H2 type of hysteresis loop according to IUPAC which means the pore character of materials which have more complex pore structures and until relative pressure is decreased to allow evaporation from the neck, the liquid seems to be trapped in the body of the pore [46].

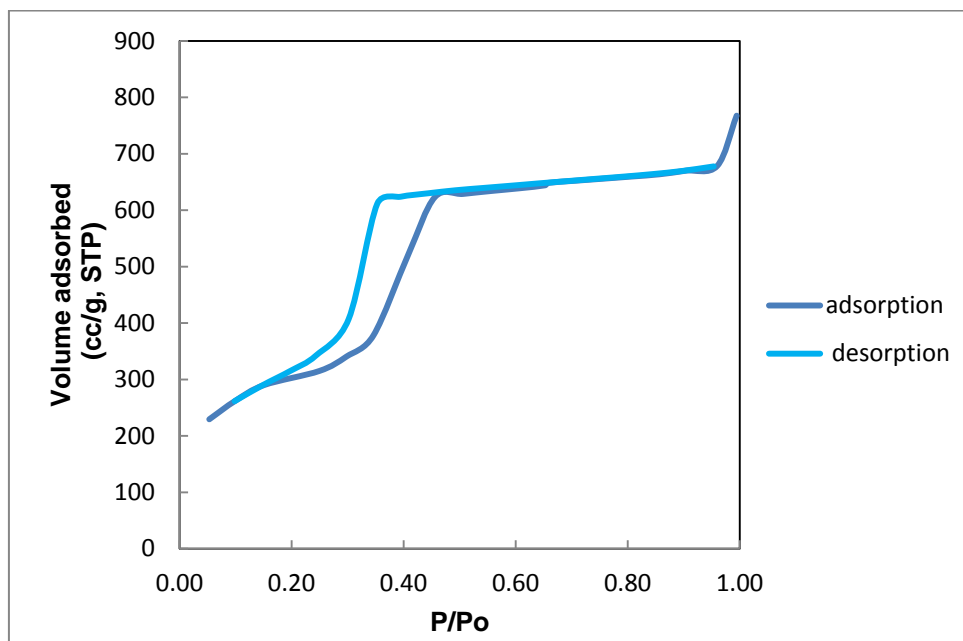


Figure 4.2: Nitrogen physisorption isotherm of synthesized MCM-41

BET surface area, pore volume and pore diameter values of calcined MCM-41 sample are listed in Table 4.1. It is clearly seen from Table 4.1 surface area of the MCM-41 sample has high surface area exceeding 1000 m²/g as stated at the literature [11]. In a previous study the BET surface area of pure MCM-41 which was synthesized by the same procedure was found as 1290 m²/g [19].

Pore size of MCM-41 sample in the mesoporous ranges. Pore size distribution curves for MCM-41 are shown in Figure 4.3. As shown in the figure, pore size distribution of MCM-41 was very narrow.

Table 4.1: Surface area, pore volume, and BJH desorption pore diameter of MCM-41 sample

Sample	Multipoint BET surface area (m ² /g)	BJH Desorption Pore Volume (cc/g)	BJH Desorption Average Pore diameter (nm)
MCM-41	1154	1.306	2.75

Also pore volume of the MCM-41 is higher than the pore volume of MCM-41 which is used in the previous study which is 0.45 cc/g [62]. In addition, nitrogen adsorption isotherm data of that sample can be found in Appendix C. Obtained micropore volume of MCM-41 in this

study from the adsorption isotherm of nitrogen was 0.566 cc/g which is the approximately half of the obtained pore volume.

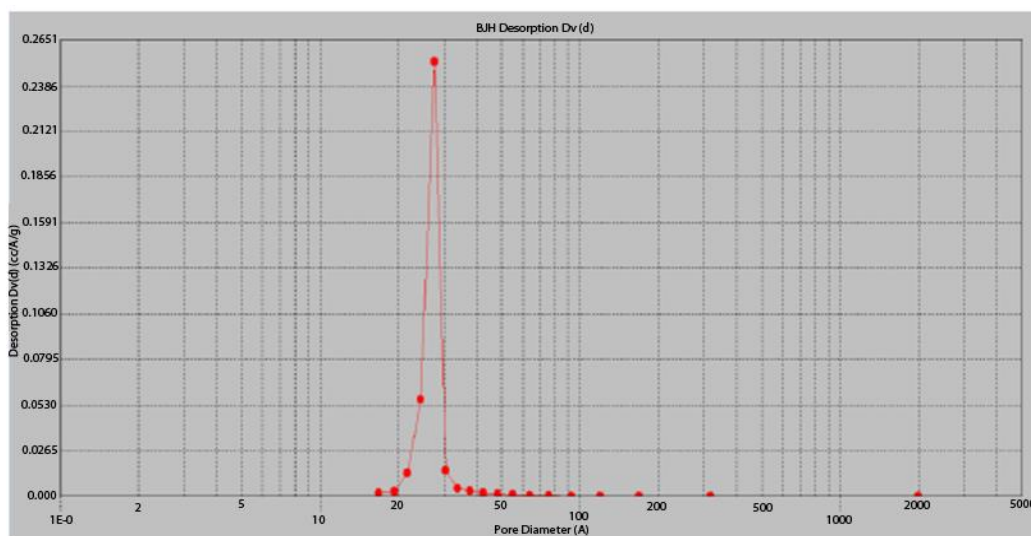


Figure 4.3: BJH desorption pore size distribution of MCM-41

4.1.3. TGA Analysis

TGA analysis was carried out by using Perkin Elmer Pyris 1 TGA in Middle East Technical University, Chemical Engineering to see at which temperature calcination should be carried out. TGA analysis for the uncalcined MCM-41 was performed under air atmosphere with a flow rate of 50 ml/min and a constant heating rate of 10 °C/min, in the temperature range of 30-900 °C. TGA results are shown in Figure 4.4. As seen in the figure water removed from the solid about 200 °C and the peak at the 310,9 °C showed the removal of organic template from the structure. Therefore, 540 °C is proper for calcination. After the removal of water and surfactant from the structure weight loss is 57.189 %.

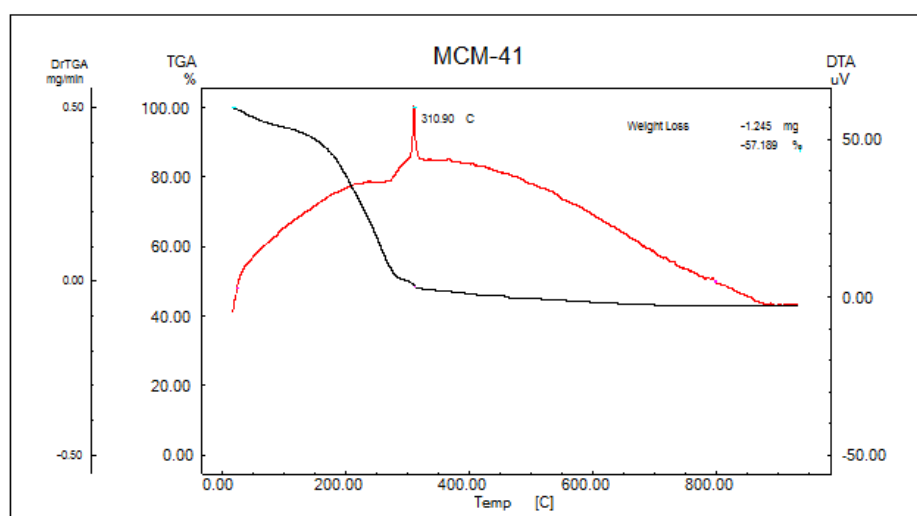


Figure 4.4: TGA analysis of uncalcined MCM-41

4.1.4. TEM Analysis

TEM analysis was carried out with the Jeol 2100F HRTEM at METU, Central Laboratory. Before the analysis suspension of powder sample in alcohol was dropped on the C-film grids and dried. TEM images of calcined MCM-41 are showed in Figure 4.5. From the image a, pore diameter which is 2.75 nm and the hexagonal pore structure can be seen. From the other images b and c ordered structure of pores can be seen.

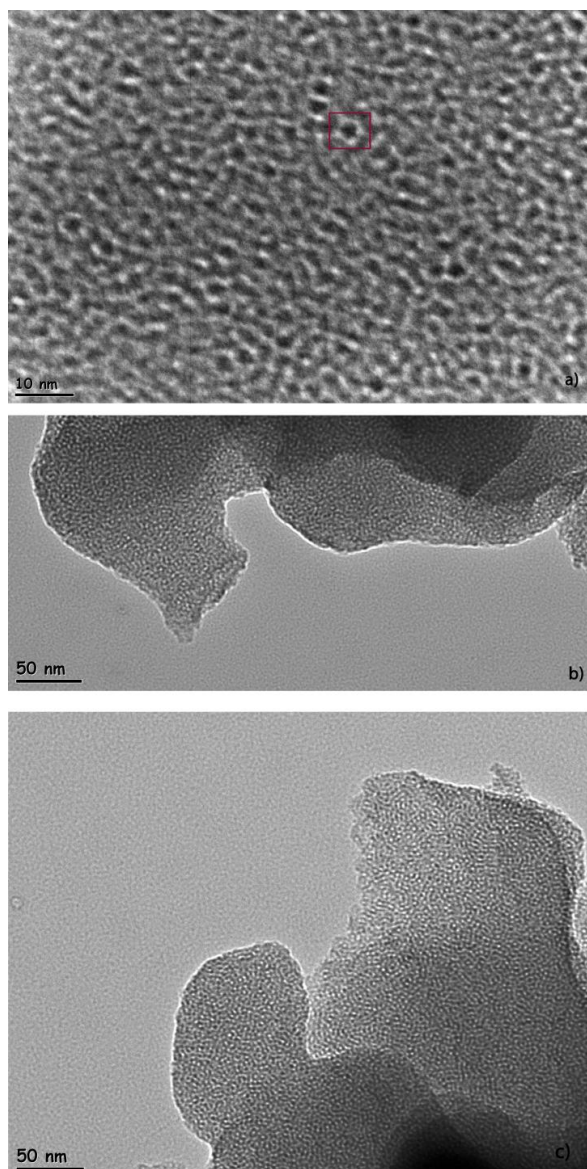


Figure 4.5: TEM images of MCM-41

However, as stated in the Chenite et al. study the equidistance parallel lines which are related to hexagonal repeat between tubules was not observed at image a) [66]. This situation may be due to while focusing 200 kV which cause defects in the structure of the sample or the synthesized MCM-41 sample was not highly ordered and has some defects on the structure. Also observed pore wall thickness from these images is not homogenous. In some areas wall thickness seems to be increased. In a previous study increase in the wall thickness in collapsed areas of the rods was a result of structural degradation [74].

4.1.5. SEM Analysis

SEM analyses were done by using FEI QUANTA 400 FE SEM, at METU, Central Laboratory. Before the analysis sample was attached on a carbon tape and coated with Au-Pd. SEM images of the synthesized MCM-41 are shown in Figure 4.6. From these images a, b and c agglomerated MCM-41 particles can be seen. There are unordered small and large agglomerated particles in the range of nm. Similar agglomerated particles were observed for an unstable sample in a previous study [74].

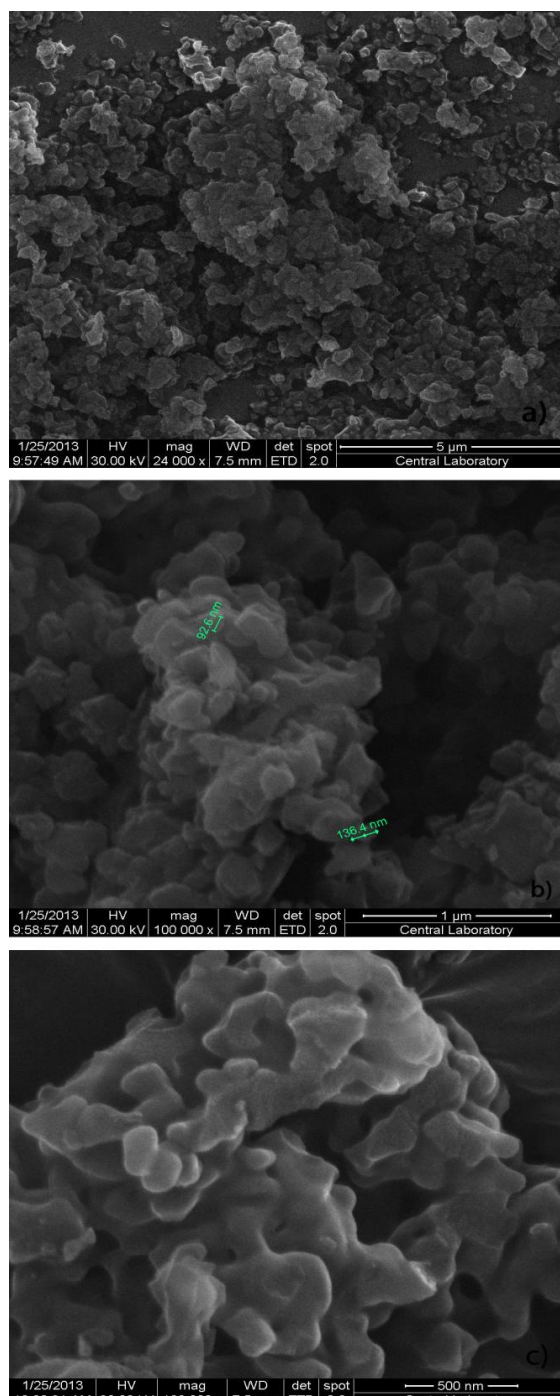


Figure 4.6: SEM images of MCM-41

4.1.6. EDX Analysis

EDX analysis of synthesized MCM-41 was carried by using FEI QUANTA 400 FE SEM, at METU, Central Laboratory. Chemical composition of the synthesized sample is listed in Table 5.2 and EDX of the sample is given in the Figure 4.7. Peaks for the Si and O atoms can be seen from the EDX analysis of the MCM-41 sample. According to atomic analysis obtained from EDX oxygen atomic concentration is 66.40% and silicium atomic concentration is 33.60%. These results showed that the structure of the synthesise material was in pure SiO_2 form.

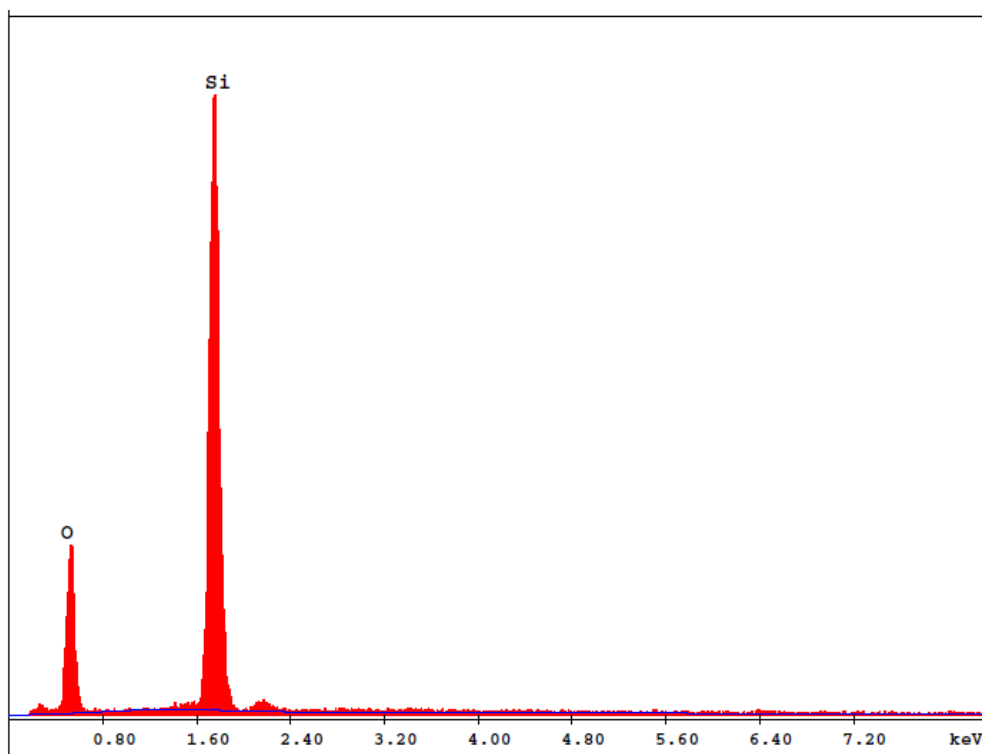


Figure 4.7: EDX analysis of MCM-41

Table 4.2: Elemental EDX analysis of MCM-41

Element	Weight %	Atomic %
O	52.96	66.40
Si	47.04	33.60

4.2. Adsorption of p-xylene, m-xylene, and o-xylene on MCM-41

Adsorption isotherms of p-xylene, m-xylene and o-xylene on MCM-41 sample, which is synthesized and characterized in this study, were investigated at 30 °C, 50 °C and 65 °C. Kinetic diameter of these isomers are listed in Table 4.3

Table 4.3: Kinetic diameters of xylenes [67]

Isomer	Kinetic Diameter (Å)
p-xylene	5.85
m-xylene	6.2
o-xylene	6.8

Adsorption isotherms for the xylene isomers are presented in Figures 4.8-4.16. Detailed isotherms data can be found in Appendix B.

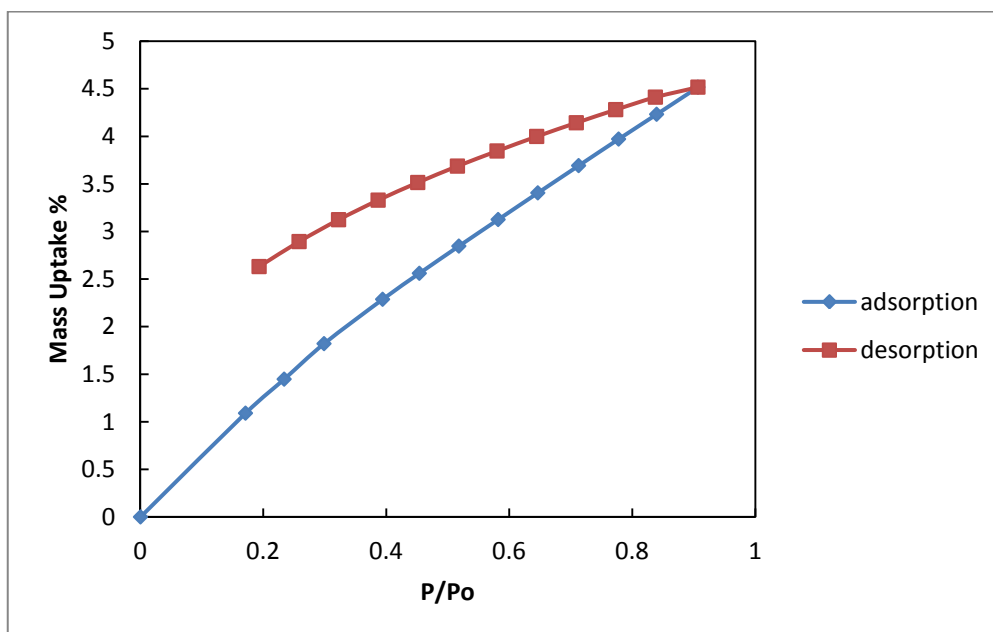


Figure 4.8: Adsorption isotherm of p-xylene at 30 °C

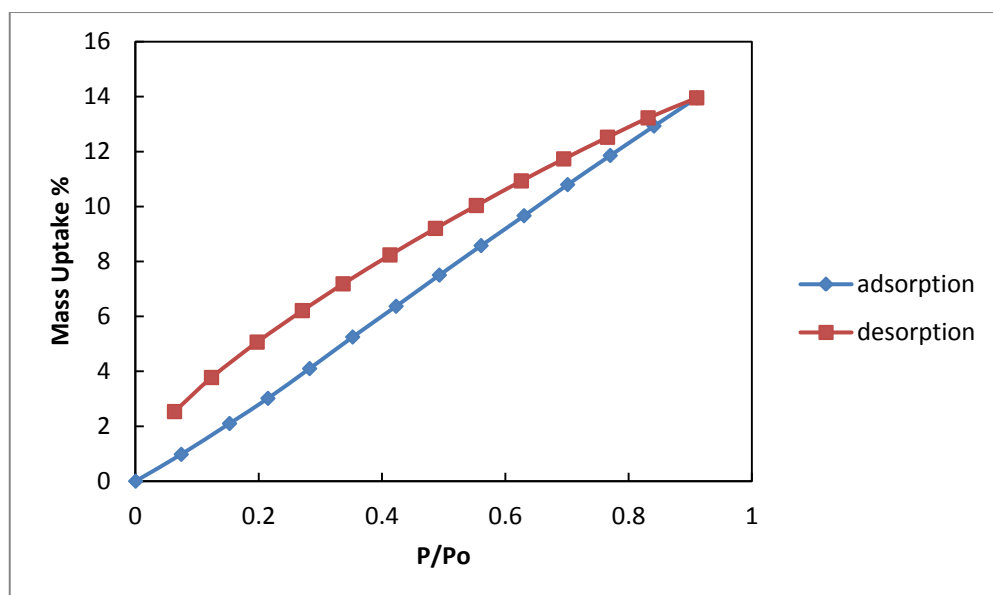


Figure 4.9: Adsorption isotherm of p-xylene at 50 °C

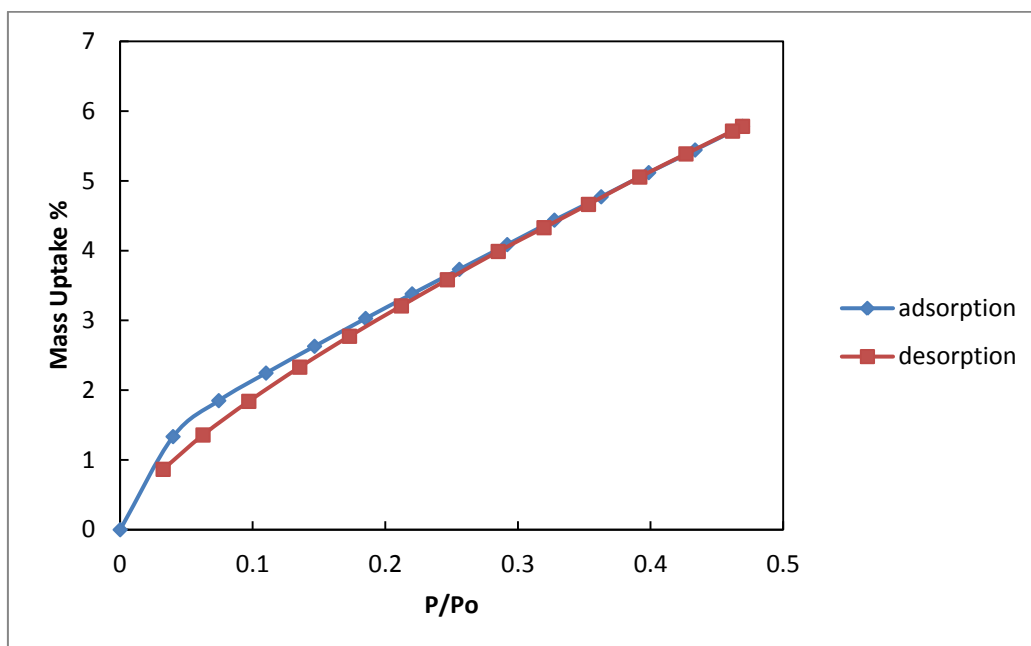


Figure 4.10: Adsorption isotherm of p-xylene at 65 °C

While high relative pressure can be reached at 30 °C and 50 °C, at 65 °C maximum relative pressure reached was lower because maximum temperature of the “Anti-condensation system” is 50 °C and the pressure of this chamber should be kept below the vapor pressure of the sorbates at 50°C to prevent condensation in this chamber.

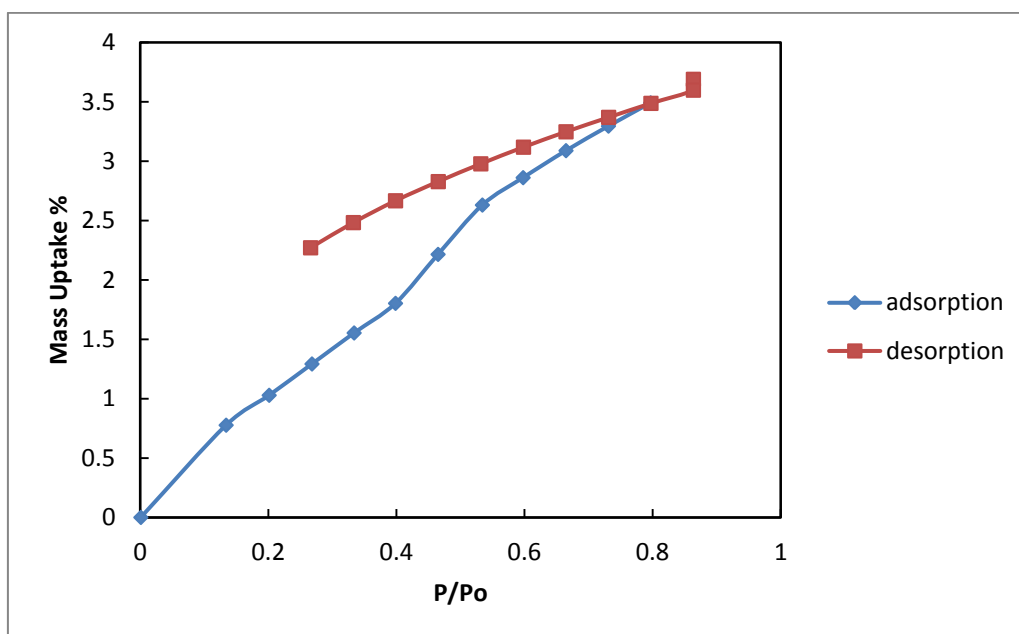


Figure 4.11: Adsorption isotherm of m-xylene at 30 °C

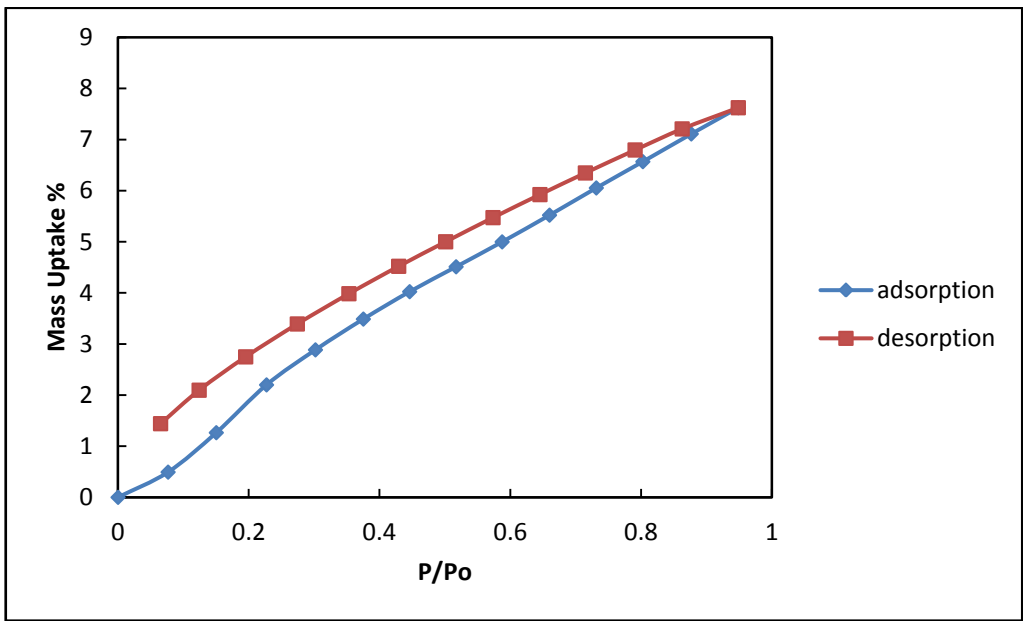


Figure 4.12: Adsorption isotherm of m-xylene at 50 °C

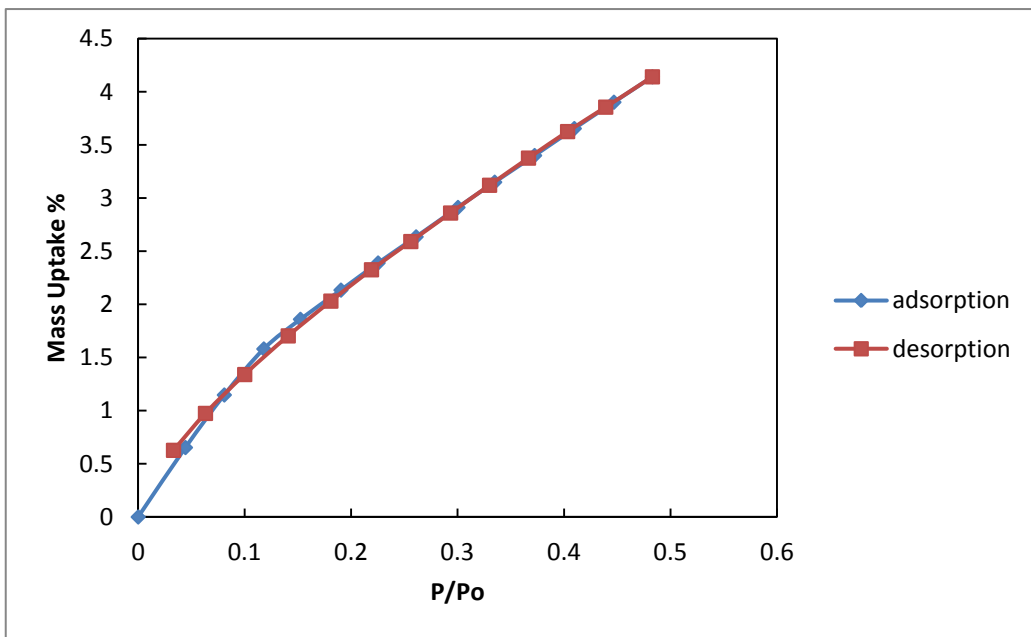


Figure 4.13: Adsorption isotherm of m-xylene at 65 °C

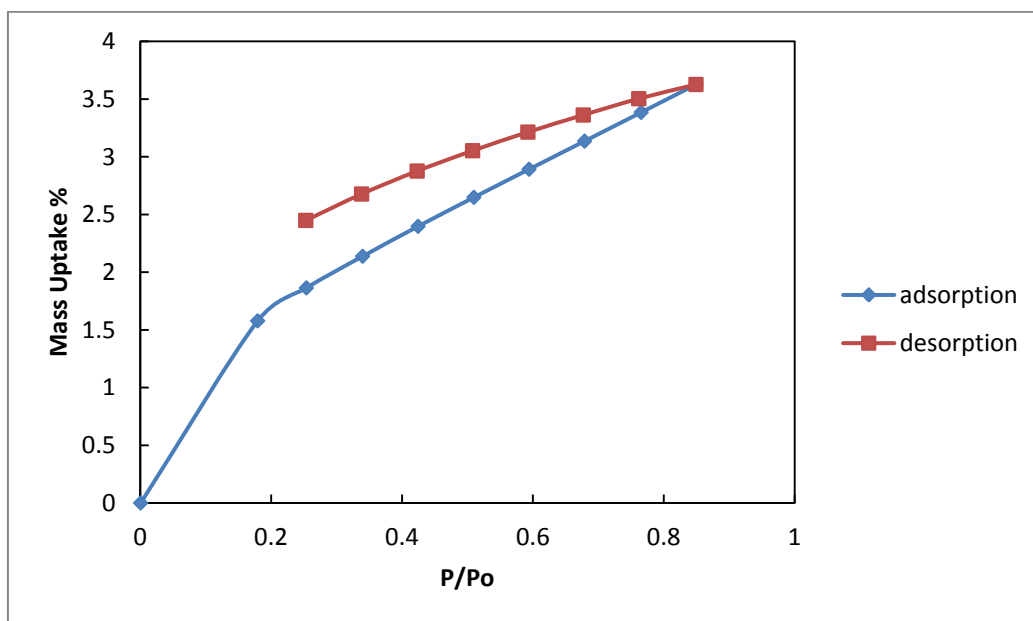


Figure 4.14: Adsorption isotherm of o-xylene at 30 °C

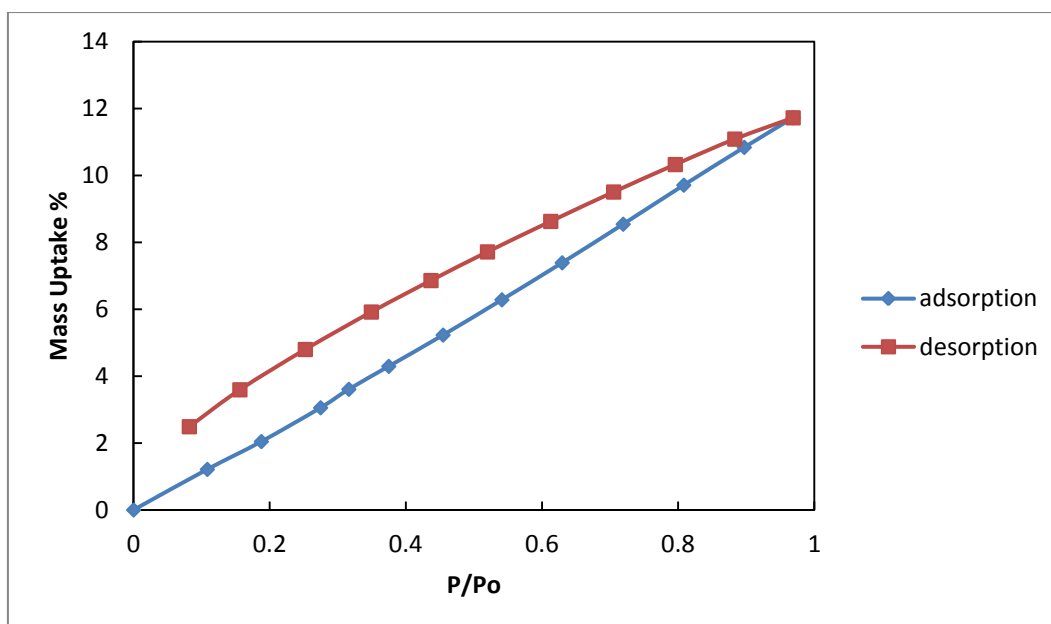


Figure 4.15: Adsorption isotherm of o-xylene at 50 °C

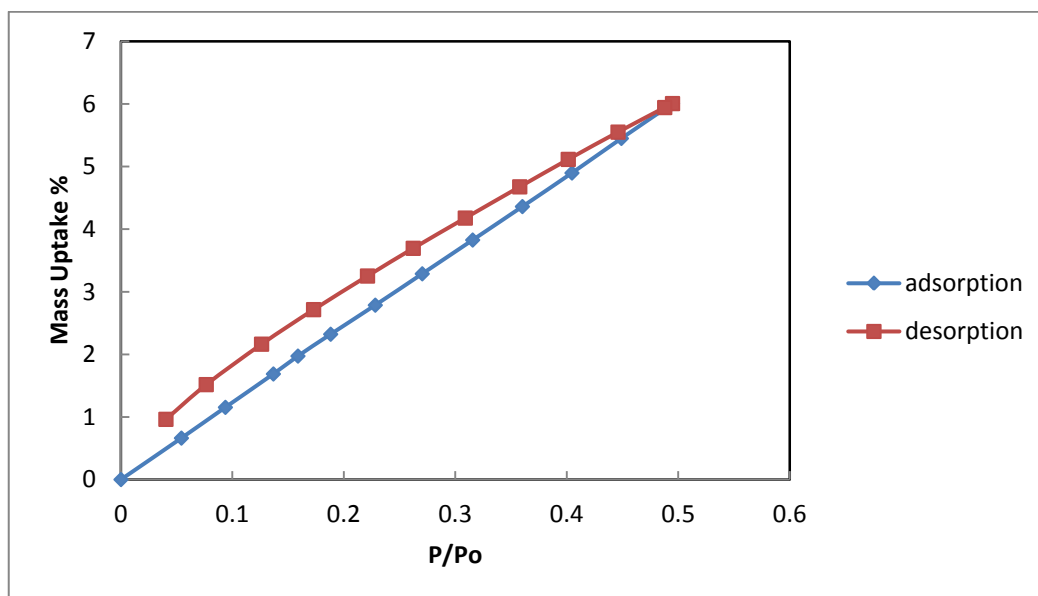


Figure 4.16: Adsorption isotherm of o-xylene at 65 °C

Detailed sorption isotherms data of this work can be found in Appendix B. Equilibrium sorption capacities for p-xylene, m-xylene and o-xylene listed in the Table 4.4, 4.5 and 4.6 respectively. Equilibrium sorption capacities in this study are lower than those found in a previous study done with the same adsorbates and conditions on a MCM-41 sample with lower surface area and pore volume. Capacities of that study can be found in Appendix C. In that study used MCM-41 sample was synthesized by hydrothermal method like the sample that was used in this study. For both samples surfactants are CTMABr, however silica sources are different. In this study silica source is TEOS which is acidic. On the other hand, silica source in the previous study is sodium silicate which is basic [62]. For both samples in the synthesis procedure pH was adjusted to 11. For pH adjustment in this study NaOH was used, in previous study H₂SO₄ was used. Resultant MCM-41 sample in this study has higher surface area and pore volume, but sorption capacities of xylenes are lower.

Table 4.4: Equilibrium sorption capacities of p-xylene

Temperature (°C)	Max. Relative Pressure	Mass Uptake %
30	0.907	4.517
50	0.910	13.955
65	0.469	5.782

Table 4.5: Equilibrium sorption capacities of m-xylene

Temperature (°C)	Max. Relative Pressure	Mass Uptake %
30	0.863	3.689
50	0.948	7.623
65	0.483	4.141

Table 4.6: Equilibrium sorption capacities of o-xylene

Temperature (°C)	Max. Relative Pressure	Mass Uptake %
30	0.849	3.627
50	0.969	11.724
65	0.495	6.006

As seen from the Tables 4.7, 4.8 and 4.9 the total adsorbed amount for all isomers at the same pressure decreases as the temperature of the adsorption isotherms increases. The decrease of adsorbed amount is because of the decrease of density of the sorbates with the increasing temperature. For hexane adsorption on MCM-41, Qiao et al. observed same behavior [68]. Also the previous study done about the sorption capacities of C₈ aromatics on MCM-41 showed the same observation [62].

According to adsorption isotherms, p-xylene adsorbed amount on MCM-41 sample was higher than the m-xylene and o-xylene.

Table 4.7: Sorption capacities of p-xylene at similar pressure values

Temperature (°C)	Pressure (mbar)	Total Mass (mg)	Mass Uptake%
30	12.079	22.460	4.231
50	12.153	22.433	4.098
65	12.351	21.671	2.629

Table 4.8: Sorption capacities of m-xylene at similar pressure values

Temperature (°C)	Pressure (mbar)	Total Mass (mg)	Mass Uptake%
30	11.992	21.824	3.491
50	12.607	21.732	2.885
65	12.472	21.496	1.859

Table 4.9: Sorption capacities of o-xylene at similar pressure values

Temperature (°C)	Pressure (mbar)	Total Mass (mg)	Mass Uptake%
30	9.035	21.823	3.384
50	9.247	21.745	3.055
65	9.183	21.470	1.687

In a previous study, adsorption isotherms of p-xylene, m-xylene and o-xylene found as type V according to IUPAC classification [62]. In addition the xylenes adsorption on HZSM-35 zeolite was found type I due to microporous nature of the adsorbent [67]. Besides these studies, N₂ adsorption of MCM-41 in this study shows type IV characteristic with H2 type hysteresis loop. However, for all adsorbates an approximate linear increase in the adsorption amount was observed from the adsorption isotherms. Except for adsorption isotherms of m-xylene and p-xylene at 65 °C all isotherms show hysteresis loops.

The H2 type adsorption hysteresis is explained as a consequence of the interconnectivity of pores. In such systems, the distribution of pore sizes and the pore shape is not well-defined or irregular. A sharp step on the desorption isotherm is usually understood as a sign of interconnection of the pores. If a pore connected to the external vapor phase via a smaller pore, in many cases the smaller pore acts as a neck (often referred to as an "ink-bottle" pore [69]).

Hysteresis loops associated with capillary condensation. The desorption occurs via evaporation of the adsorbate from mesopores and usually takes place at a relative pressure

lower than that of capillary condensation. Condensation takes place at relative pressure provided by the Kelvin equation, but evaporation from the pore body cannot occur while the pore mouth remains filled [70]. The presence and size of the hysteresis loops depend on the adsorbate, pore size and temperature [10]. The hysteresis is, in general, attributed to the different sizes of the pore mouths and pore bodies or to the different adsorption and desorption behaviors in near-cylindrical pores. In MCM-41 sample, pores are believed to be very long compared to their diameters. It is then very likely that the radius is not constant as the pore length, but rather there may be some constrictions caused by imperfections of the pore wall [71].

As seen from the adsorption isotherm figures hysteresis loops getting narrower with the increasing temperature. As the temperature increase the capillary condensation steps shift from low to high relative pressures. The large shift of the phase transition from low to high relative pressures originates from the decrease of the surface tension as temperature increase, that is, it needs higher pressure to achieve the capillary adsorption phase transition at the lower surface tension [68]. This shift may cause the reversible adsorption isotherms of m-xylene and p-xylene at 65 °C.

The volume of sorbates (V_p) was determined from the amounts adsorbed at maximum relative pressure with the assumption pores are filled with condensed sorbate in the normal liquid state. Determined volume listed in Tables 4.10-4.12.

Table 4.10: The adsorbed volumes (V_p) of p-xylene

Temperature (°C)	Max. Relative Pressure (P/Po)	Density (g/cm ³)[62]	Mass Uptake %	V_p (cm ³ /g)
30	0.907	0.852	4.517	0.053
50	0.910	0.836	13.955	0.167
65	0.469	0.822	5.782	0.070

Table 4.11: The adsorbed volumes (V_p) of m-xylene

Temperature (°C)	Max. Relative Pressure (P/Po)	Density (g/cm ³)[62]	Mass Uptake %	V_p (cm ³ /g)
30	0.863	0.855	3.689	0.043
50	0.948	0.838	7.623	0.091
65	0.483	0.825	4.141	0.050

Table 4.12: The adsorbed volumes (V_p) of o-xylene

Temperature (°C)	Max. Relative Pressure (P/Po)	Density (g/cm ³)[62]	Mass Uptake %	V_p (cm ³ /g)
30	0.849	0.870	3.627	0.042
50	0.969	0.853	11.724	0.137
65	0.495	0.839	6.006	0.072

At the maximum relative pressures for p-xylene, m-xylene and o-xylene which are 0.910, 0.948 and 0.969 respectively determined volume of liquid sorbates are significantly lower according to pore volume (1.306 cm³/g) determined by nitrogen adsorption at 77K. This shows that pores were filled with low amount of adsorbates. Therefore, equilibrium capacities of xylenes are very low when compared to early study [62].

4.3. Adsorption of Ethylbenzene on MCM-41

The sorption capacities of ethylbenzene on MCM-41 at 30 °C, 50 °C and 65 °C were determined and listed in Table 4.13. Ethylbenzene has kinetic diameter (6.0 Å) [67]. Adsorption isotherms of ethylbenzene at 30 °C, 50 °C and 65 °C are shown in Figures 4.17-4.19 also detailed experiment data can be found in Appendix B.

Table 4.13: Equilibrium sorption capacities of ethylbenzene

Temperature (°C)	Max. Relative Pressure	Mass Uptake %
30	0.900	4.779
50	0.961	13.055
65	0.520	6.856

As seen from the Figures 4.18 and 4.19, adsorption isotherms of ethylbenzene at 50 °C and 65 °C are reversible, not giving hysteresis loop. On the other hand, at 30 °C hysteresis loop is observed. The adsorption isotherms of m-xylene and p-xylene at 65 °C showed similar characteristic. As the temperature increase the capillary condensation steps shift from low to high relative pressures and therefore for higher temperatures reversible isotherms were observed [68]. In addition, the linear increase in the adsorption amount of ethylbenzene was observed similar to adsorption isotherms of xylenes on the same sample.

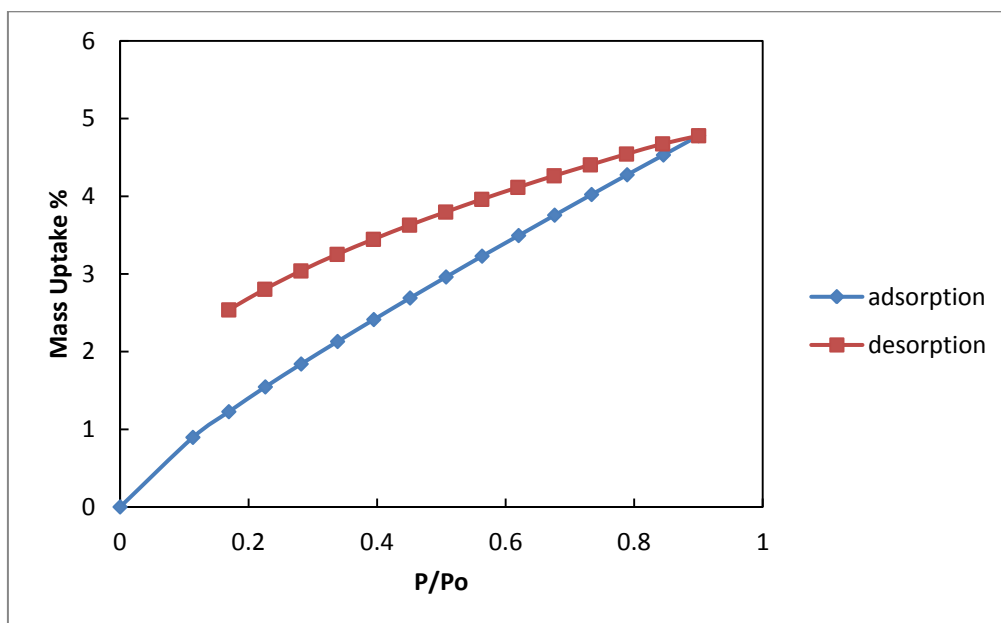


Figure 4.17: Adsorption isotherm of ethylbenzene on MCM-41 at 30 °C

The repetition of the adsorption isotherm of ethylbenzene at 30 °C shows the obtained data are reproducible. This repeated adsorption isotherm detailed data can be found in Appendix B.

For the adsorption data at 65 °C maximum relative pressure can not be reached because of the temperature limitation of the “Anti-condensation system”. Maximum temperature of the “Anti-condensation system” is 50 °C and the pressure of this chamber should be kept below the vapor pressure of the sorbates at 50°C to prevent condensation in this chamber.

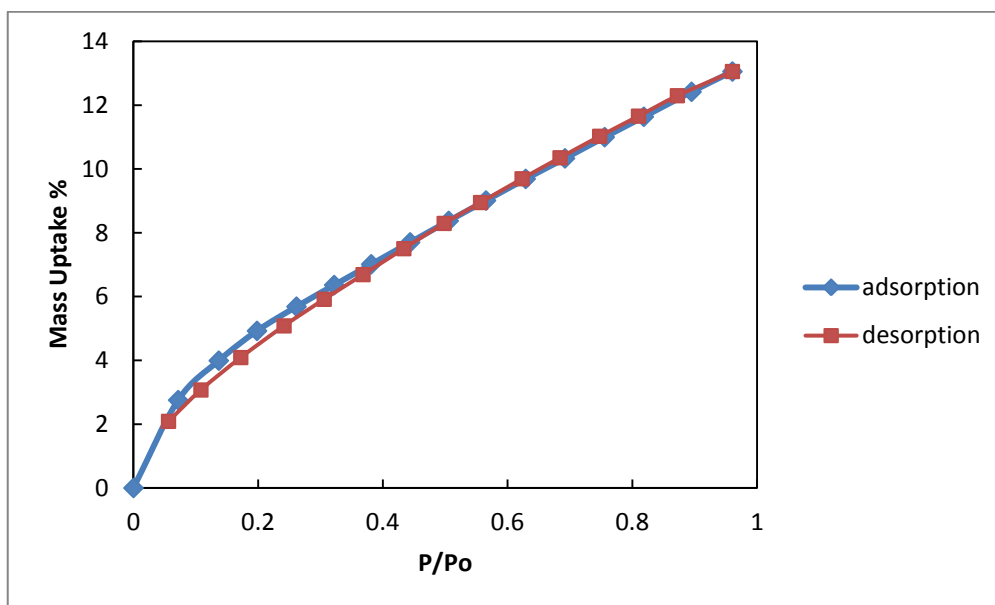


Figure 4.18: Adsorption isotherm of ethylbenzene on MCM-41 at 50 °C

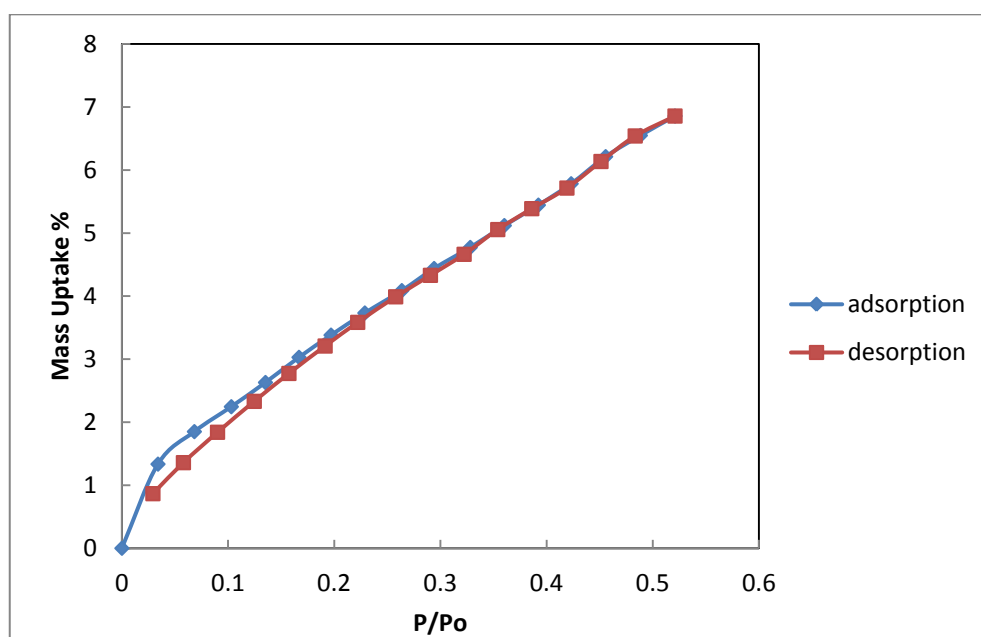


Figure 4.19: Adsorption isotherm of ethylbenzene on MCM-41 at 65 °C

The volume of ethylbenzene was determined from the amounts adsorbed at maximum relative pressure with the assumption pores are filled with condensed sorbate in the normal liquid state.

Table 4.14: The adsorbed volumes (V_p) of ethylbenzene

Temperature (°C)	Relative Pressure (P/P ₀)	Density (g/cm ³)[62]	Mass Uptake %	V _p (cm ³ /g)
30	0.900	0.859	4.779	0.056
50	0.961	0.633	13.055	0.206
65	0.520	0.828	6.856	0.083

At maximum relative pressure which was reached at 50 °C the volume of liquid sorbate amount was calculated as 0.206 cm³/g which is significantly lower than that obtained from low-temperature nitrogen isotherm (1.306 cm³/g).

In this study determined equilibrium sorption capacities of ethylbenzene on the MCM-41 sample were lower than capacities in a previous study as well as xylenes [62]. Obtained sorption capacities in the previous study can be found in Appendix C. Although the MCM-41 sample in this study has high surface area and pore volume which make it proper to use as adsorbent, adsorption of C₈ aromatics on this sample was unexpectedly low. According to characterization of this sample, this low adsorption may be due to structural degradation [74]. From the TEM images increasing wall thickness in the collapsed area of the rods can be observed and also from the XRD pattern obtained wall thickness is 4.67 nm.

CHAPTER 5

CONCLUSION AND RECOMMENDATIONS

The aim of this study is to determine the sorption capacities of p-xylene, m-xylene and o-xylene on MCM-41 type of mesoporous material which was synthesized in this study with CTAMBr (as surfactant) and TEOS (as silica source). For this purpose by using IGA system which is an automated gravimetric electro balance system, at different temperatures that are 30°C, 50°C and 65 °C isotherm data was observed. To investigate also sorption capacity of ethylbenzene on the MCM-41 that is used in this study, isotherm data at 30 °C, 50°C and 65 °C were studied.

MCM-41 sample was synthesized by hydrothermal synthesis method with CTAMBr (surfactant) and TEOS (silica source) in basic conditions. This MCM-41 was calcined at 540 °C for 8 h and characterized by XRD, nitrogen adsorption analysis, TGA, TEM, SEM and EDX. The characterization results indicated that desired structure of MCM-41 in SiO₂ form was successfully synthesized with high surface area and pore volume. It can be concluded that synthesized MCM-41 have required features to be used as adsorbent.

Adsorption of p-xylene, m-xylene, o-xylene were investigated on synthesized MCM-41 at 30 °C, 50 °C and 65 °C by using IGA system. The total adsorbent amount for all isomers at the same pressure decreased as the temperature of the adsorption isotherms increases. For the 65 °C high relative pressures cannot be reached due to temperature limitation of "Anti-condensation" system. For all adsorbates the linear increase in the adsorption amount was observed from the adsorption isotherms. Isotherms do not fit IUPAC classification types for mesoporous materials. On the other hand nitrogen adsorption at 77 K on this MCM-41 shows type IV and H2 hysteresis loop characteristics.

Except for adsorption isotherms of m-xylene and p-xylene at 65 °C all isotherms of xylenes show hysteresis loops. Ethylbenzene adsorption isotherms were determined at 30°C, 50 °C and 65 °C. They showed a linear increase in the adsorption amount like xylenes and for 50 °C and 65 °C reversible without a hysteresis loop. However for 30°C, hysteresis loop was observed. Hysteresis loops getting narrower with the increasing temperature. For all adsorbates volume adsorbed calculated and found significantly low when compared to pore volume obtained from nitrogen adsorption. Obtained adsorption capacities of these hydrocarbons on MCM-41 are very low when compared to previous study.

Sorption capacities of these aromatic hydrocarbons on MCM-41 sample which was synthesized in this study are low although this sample has high surface area and pore volume. These low adsorption capacities may be due to structure degradation. Therefore, adsorption capacities can be studied on other MCM-41 samples which are synthesized with same method and have more ordered structure to see what cause the low sorption capacity structure degradation or adsorbent-adsorbate interaction.

REFERENCES

1. Zhao, X. S., Lu, G. Q., Millar, G. J., "Advances in mesoporous molecular sieve MCM-41", *Ind. Eng. Chem. Res.*, 1996, 35, 2075-2090.
2. Alatham, Z.A, "A Review: Fundamental Aspects of Silicate Mesoporous Materials, Materials", 2012, 5, 2874-2902
3. Melo, R. A. A., Giotto, M. V., Rocha, J., Gonzalez, E. A., "MCM-41 ordered mesoporous molecular sieves synthesis and characterization", *Materials Research*, 1999, 2, 173-179.
4. Hoffmann, F., Cornelius, M., Morell, J., Fröba, M., "Silica-based Mesoporous Organic-Inorganic Hybrid Materials," *Angew. Chem. Int. Ed*, 2006, 45, 3216-3251
5. Selvam, P., Bhatia, S. K., Sonwane, C. G., "Recent advances in processing and characterization of periodic mesoporous MCM-41 silicate molecular sieves", *Ind. Eng. Chem. Res.*, 2001, 40(15), 3237-3261
6. Vartuli, J. C., Malek, A., Roth, W. J., Kresge C. T., McCullen, S. B., "The sorption properties of as-synthesized and calcined MCM-41 and MCM-48, *Microporous and Mesoporous Materials*", 2001, 44-45, 691-695.
7. Vartuli, J.C., Shih, S.S., Kresge, C.T., Beck, J.S., "Potential Applications for M41S Type Mesoporous Molecular Sieves", *Mesoporous Molecular Sieves*, 1998, Vol. 117.
8. Santos, K. A. O., Dantas Neto, A. A., Moura, M. C. P. A., Castro Dantas, T. N., "Separation of xylene isomers through adsorption on microporous materials: A review", *Brazilian Journal of Petroleum and gas*, v. 5 ,n. 4 ,p. 255-268 ,2011, ISSN 1982-0593
9. Guo, G. Q., Chen, H., Long, Y.C., "Separation of p-xylene from C8 aromatics on binder-free hydrophobic adsorbent of MFI zeolite. I. Studies on static equilibrium", *Microporous and Mesoporous Materials*, 39, 2000, 149-161
10. Ciesla, U., Schüth, F. (1999). "Ordered mesoporous materials", *Microporous and Mesoporous Materials* 27, p.131-149
11. Sayari, A. (1996). "Periodic mesoporous materials: synthesis, characterization and potential applications", *Recent Advances and New Horizons in Zeolite Science and Technology Studies in Surface Science and Catalysis* 102, p.1-46
12. Güçbilmez, Y., "Vanadium and Molybdenum Incorporated MCM-41 Catalysts for Selective Oxidation of Ethanol", *Master Thesis, METU*, 2005.
13. Roth, W. J. and Vartuli, J. R. (2005) "Synthesis of mesoporous molecular sieves", *Studies in Surface Science and Catalysis* 157, p.91-110.
14. Corma, A., "From microporous to mesoporous molecular sieve materials and their use in catalysis", *Chem. Rev.*, 1997, 97, 2373-2419
15. Oye, G., Sjöblom, J., Stöcker, M., "Synthesis, characterization and potential applications of new materials in the mesoporous range, *Advances in Colloid and Interface Science*", 2001, 89-90, 439-466.
16. Yanagisawa, T.; Schimizu, T.; Kiroda, K.; Kato, C. "The Preparation of Alkyltrimethylammonium- Kanemite Complexes and their Conversion to Mesoporous Materials", *Bull. Chem. Soc. Jpn.*,1990, 63, 988-992.
17. Beck, J. S., Vartuli, J. C., Roth, W. J., Leonowicz, M. E., Kresge, C. T., Sheppard, E. W., McCullen, S. B., Higgins, J. B., Schlenker, J. L., "A new family of mesoporous molecular sieves prepared with liquid crystal templates", *J. Am. Chem. Soc.*, 1992, 114, 10834-10843
18. Kresge, C. T., Leonowicz, M. E., Roth, W. J., Vartuli, J. C., Beck, J. S. (1992). "Ordered mesoporous molecular sieves synthesized by a liquid-crystal template mechanism", *Nature* 359, p.710-712

19. Aydemir, B., " Synthesis of Mesoporous Catalysts and Their Performance in Pyrolysis of Polyethylene, Master Thesis, METU, 2010.
20. Beck, J.S.; Calabro, D.C.; McCullen, S.B.; Pelrine, B.P.; Schmitt, K.D.; Vartuli, J.C. "Method for Functionalizing Synthetic Mesoporous Crystalline Material". U.S. Patent 2,069,722, 27 May 1992
21. Vartuli, J.C.; Roth, W.J.; Degnan, T.F. "Mesoporous materials (M41S): From discovery to Application". In Dekker Encyclopedia of Nanoscience and Nanotechnology; Schwarz, J.A.,Contescu, C.I., Putyera, K., Eds.; Taylor and Francis: New York, NY, USA, 2008; pp. 1797–1811
22. Zhai, Q. Z., Wang, P., "Preparation, characterization and optical properties of lanthanum-(nanometer MCM-41) composite materials", J. Iran. Chem. Soc., 2008, 5, 268-273.
23. Karge, H.G., Weitkamp, J., "Molecular sieves synthesis" 1st edition, Springer-Verlag, Newyork, 97-118 (1998).
24. Sener, C., "Synthesis and characterization of Pd-MCM-Type mesoporous nanocomposite materials", Master Thesis, METU, 2007
25. Collart, O., "Nanodesign of an Aluminasilicate Framework in Mesoporous MCM-48 Architecture", PhD Thesis, University of Antwerpen, 2003
26. Stucky, G. D., MacDougall, J. E., "Quantum confinement and host/guest chemistry: Probing a new dimension, Science", 1990, 247, 669-678
27. Anderson, M. W., "Simplified description of MCM-48 Zeolites", 1997, 19, 220-227
28. Roth, W. J., Synthesis of the Cubic Mesoporous Molecular Sieve MCM-48, 2000, US Patent No. 6, 096, 288
29. Glanville, Y. J., Pearce, J. V., Sokol, P. E., Newalker, B., Komarneni, S., "Study of H₂ confined in highly ordered pores of MCM-48", Chemical Physics, 292: 289-293 (2003)
30. Behrens, P., Glaue, A., Haggemüller, C., Schechner, G., Structure-directed materials synthesis: Synthesis field diagrams for the preparation of mesostructured silicas, Solid State Ionics, 1997, 101-103, 255-260
31. Jana, K. S., Nishida, R., Shindo, K., Kugita, T., Namba, S., "Pore size control of microporous molecular sieves using different organic auxiliary chemicals", Microporous and Mesoporous Materials, 2004, 68, 133-142
32. Myers, D., "Surfactant Science and Technology", 2nd ed., 1992, 28, 7, 936
33. Monnier, A.; Schüth, F.; Huo, Q.; Kumar, D.; Margolese, D.; Maxwell, R.S.; Stucky, G.D.; Krishnamurty, M.; Petroff, P.; Firoouzi, A.; Janicke, M.; Chmelka, B.F. "Cooperative formation of inorganic–organic interfaces in the synthesis of silicate mesostructures". Science 1993, 261, 1299–1303.
34. Karakassides, M.A.; Bourlinos, A.; Petridis, D.; Coche-Guerente, L.; Labbe, P. Synthesis and characterization of copper containing mesoporous silicas. J. Mater. Chem. 2000, 10, 403–408.
35. Hunter, R.J., "Introduction to Modern Colloid Science", Oxford University Press, New York; 1993
36. Ying, J., Mehnert, C.P., and Wong, M.S., Angew. Chem. Int. Ed., 38, (1999), 56
37. Chen, C. Y., Li, H. Y., Davis, M. A., "Studies on mesoporous materials II: Synthesis mechanism of MCM-41", Microporous Mater., 1993, 2, 27.
38. Gao, C., "Formation mechanism of anionic-surfactant-templated mesoporous silica (AMS)", Master Thesis, Stockholm University, 2009
39. Sonwane, C. G., Bhatia, S.K., "Structural characterization of MCM-41 over a wide range of length scales", Langmuir, 1999, 15, 2809-2816
40. Arinan, A., "Direct synthesis of dimethyl ether (dme) from synthesis gas using novel catalysts, Master Thesis", METU, 2010
41. Sing, K., "Physisorption of nitrogen by porous materials, Journal of Porous Materials", 1995, 2, 5-8

42. Wang, W., Song, M., "Preparation of high nickel-containing MCM-41 type mesoporous silica via a modified direct synthesis method", *Materials*, 2005, 20, 1737-1744.
43. Guo, X., Lai, M., Kong, Y., Ding, W., Yan, Q., "Novel coassembly route to Cu- SiO₂ MCM-41-like mesoporous materials", *Langmuir*, 2004, 20, 2879-2882
44. Vartuli, J. C., Shih, S.S., Kresge, C. T., Beck J.S., "Potential applications for M41S type mesoporous molecular sieves", *Mesoporous Molecular Sieves*, 1998, 117,
45. Corma, A., Fornes, V., Garcia, H., Miranda, M. A., Sabater, M.J., "Highly Efficient Photoinduced Electron Transfer with 2,4,6-Triphenylpyrylium Cation Incorporated inside Extra Large Pore Zeotype MCM-41", *J Am Chem Soc*, 116 (21) (1994), pp. 9767–9768
46. IUPAC Recommendations, *Pure Appl. Chem.*, Vol. 57 (1985), 603-619
47. Isotherm classifications. Prof. Dr. Marc Donohue, Department of Chemical Engineering, Johns Hopkins University
48. Rouquerol, F., Rouquerol, J., Sing, K., "Adsorption by Powders and Porous Solids: Principles, Methodology and Applications II", Academic Press, United Kingdom, 1999
49. Özşin, G., Production and Characterization of Activated Carbon From Pistachio-nut Shell, Master Thesis, METU, 2011
50. Branton, P. J., Hall, P.G., Sing K.S.W., "Physisorption of Argon, Nitrogen and Oxygen by MCM-41, a Model Mesoporous Adsorbent", *J. Chem. Soc. Faraday Trans.*, 1994, 90(19), 2965-2967.
51. Rathousky, J., Zukal, A., "Adsorption on MCM-41 Mesoporous Molecular Sieves, Part 1 Nitrogen Isotherms and Parameters of the Porous Structure", *J. Chem. Soc. Faraday Trans.*, 1994, 90(18), 2821-2826.
52. Branton, P. J., Hall, P. J., and Sing, S. W. K., "Physisorption of alcohols and water vapour by MCM-41, a model mesoporous adsorbent". *Adsorption*, 1, 77-82 (1995).
53. Choma J, Kloske, M., "Benzene adsorption isotherms on MCM-41 and their use for pore size analysis", *Adsorption*, 10: 195-2003, 2004
54. Ribiero Carrott, M.M.L., Candeias, A.J.E., Carrott, P.J.M., Ravikovitch, P.I., Neimark, A.V., Sequeira, A.D., "Adsorption of nitrogen, neopentane, n-hexane, benzene and methanol for the evaluation of pore sizes in silica grades of MCM-41", *Microporous and Mesoporous Materials*, 47, 2001, 323-337
55. Qin, Q., Ma, J., Liu, K., "Adsorption of nitrobenzene from aqueous solution by MCM-41", *Journal of Colloid and Interface Science*, 315, 2007, 80–86
56. Russo, P. A., Manuela, M., Carrott, L. R., Carrott, P. J. M., "Adsorption of toluene, methylcyclohexane and neopentane on silica MCM-41", *Adsorption*, 2008, 14: 367-375
57. Huang, L., Huang, Q., Xiao, H., Eic, M., "Effect of cationic template on the adsorption of aromatic compounds in MCM-41", *Microporous and Mesoporous Materials*, 98, 2007, 330-338
58. Mangrulkar, P. A., Kamble, S. P., Meshram, J., Rayalu, S. S., "Adsorption of phenol and o-chlorophenol by mesoporous MCM-41", *Journal of Hazardous Materials*, 160, 2008, 414–421
59. Monash, P., Majhi, A., Pugazhenti, G., " Adsorption Studies of Methylene Blue onto MCM-41", the 12th international conference of international association for computer methods and advances in geomechanics (IACMAG) 1-6 October, 2008, Goa, India.
60. Ariapad, A., Zanjanchi, M.A., Arvand, M, "Efficient removal of anionic surfactant using partial template-containing MCM-4", *Desalination*, 284, 2012, 142-149.
61. Choudhary , V. R., Mantri, K., "Adsorption of Aromatic Hydrocarbons on Highly Siliceous MCM-41", *Langmuir*, 2000, 16, 7031-7037
62. Ali, B. A., "Sorption of C₈ aromatics on MCM-41", Master Thesis, METU, 2010
63. IGA System User Manual
64. Gündüz, S., "Sorption Enhanced Ethanol Reforming Over Cobalt, Nickel Incorporated MCM-41 For Hydrogen Production", Master Thesis, METU, 2011

65. She-Tin Wong, Hong-Ping Lin, Chung-Yuan Mou, "Tubular MCM-41- supported transition metal oxide catalysts for ethylbenzene dehydrogenation reaction", *Applied Catalysis A: General* 198 (2000) 103-114
66. Chenite, A., Le Page, Y., "Direct TEM Imaging of Tubules in Calcined MCM-41 Type Mesoporous Materials", *Chem. Mater.*, 1995, 7, 1015-1019.
67. Öztin, A. " Sorption properties of a high silica zeolite ZSM-35" Master Thesis, METU, 1997
68. Qiao, S. Z., Bhatia, S. K., and Nicholson, D., "Study of Hexane Adsorption in Nanoporous MCM-41 Silica", *Langmuir*, 2004, 20, 389-395.
69. Sergej, N., "Hysteresis Phenomena in Mesoporous Materials", Universit□at Leipzig, Dissertation, 2009
70. Gregg, S. J. and Sing, K. S., "Adsorption, surface area and porosity" Academic press: London, 1967, (p. 2-121)
71. Nguyen, C., Sonwane, C. G., Bhatia, S. K., Do, D. D. "Adsorption of Benzene and Ethanol on MCM-41 Materials", *Langmuir* 1998, 14, 4950-4952.
72. Yaw's Handbook of Antoine coefficients for vapour pressure, Carl L. Yaws, Last accessed 2012.
73. Kruk, M., Jaroniec, M., "Application of large pore MCM-41 molecular sieves to improve pore size analysis using nitrogen adsorption measurements", *Langmuir*, 1997, 13, 6267-6273.
74. Landau, M. V., Varkey, S. P., Herskowitz, M., Regev, O., Pevzner, S., Sen, T., Luz, Z., "Wetting stability of Si-MCM-41 mesoporous material in neutral, acidic and basic aqueous solutions", *Microporous and Mesoporous Materials*, 33, 1999, 149-163

APPENDIX A

ANTOINE EQUATION AND COEFFICIENTS

A.1 Antoine Equation

$$\log_{10} p = A - B / (T + C) \dots \dots \dots (C.1)$$

Pressure in mmHg, T in degrees Celsius, A, B, C are Antoine coefficient which were adapted from [Yaws Handbook] for all sorbates.

Table A.1: Antoine coefficients for the sorbates [adapted from 72]

Sorbate	Coefficient A	Coefficient B	Coefficient C	Temperature Range (°C)
p-xylene	7.15471	1553.95	225.230	13.26 – 343.11
m-xylene	7.18115	1573.02	226.671	(- 47.85) – 343.90
o-xylene	7.14914	1566.59	222.596	(- 25.17) – 357.22
ethylbenzene	7.15610	1559.55	228.582	(- 94.95) – 344.02

Table A.2: Vapor pressure of sorbates at adsorption temperatures (calculated by Antoine equation)

Sorbate	Vapour pressure at 30°C (mbar)	Vapour pressure at 50°C (mbar)	Vapour pressure at 65°C (mbar)	Critical Temperature (°C)
p-xylene	15.530	42.811	84.219	343.11
m-xylene	15.049	41.738	81.832	343.90
o-xylene	11.805	33.660	67.120	357.22
ethylbenzene	17.776	48.176	93.080	344.02

APPENDIX B

ADSORPTION ISOTHERMS DATA FOR ALL SORBATES

B.1. Adsorption Isotherms Data for o-,m-,p-xylene

Table B.1: Adsorption isotherm data for p-xylene at 30°C

Pressures (mbar)	Total mass (mg)	Relative Pressure (P/Po)	Mass uptake % ((Wt - Wto)/Wto)
0.008	21.515	0.000	0.000
2.659	21.790	0.171	1.090
3.635	21.867	0.234	1.447
4.642	21.946	0.298	1.821
6.121	22.040	0.394	2.287
7.048	22.104	0.453	2.560
8.046	22.165	0.518	2.846
9.038	22.225	0.581	3.125
10.039	22.285	0.646	3.405
11.07	22.346	0.712	3.692
12.079	22.405	0.777	3.971
13.039	22.460	0.839	4.231
14.082	22.521	0.906	4.516
14.082	22.521	0.906	4.516
13.008	22.499	0.837	4.411
12.006	22.471	0.773	4.280
11.011	22.442	0.709	4.142
10.011	22.411	0.644	3.998
9.01	22.379	0.580	3.845
8.01	22.345	0.515	3.686
7.008	22.309	0.451	3.514
6.008	22.269	0.386	3.329
5.009	22.225	0.322	3.123
4.012	22.177	0.258	2.893
3.003	22.120	0.193	2.631

Table B.2: Adsorption isotherm data for p-xylene at 50 °C

Pressures (mbar)	Total mass (mg)	Relative Pressure (P/Po)	Mass uptake % ((Wt - Wto)/Wto)
0.014	21.557	0.000	0.000
3.199	21.765	0.074	0.976
6.568	22.005	0.152	2.099
9.246	22.201	0.214	3.014
12.153	22.433	0.282	4.098
15.157	22.678	0.352	5.248

18.188	22.918	0.422	6.368
21.208	23.160	0.493	7.501
24.118	23.390	0.560	8.575
27.115	23.622	0.630	9.662
30.156	23.864	0.701	10.795
33.128	24.091	0.770	11.856
36.181	24.320	0.841	12.927
39.16	24.539	0.910	13.954
39.16	24.539	0.910	13.954
35.768	24.384	0.831	13.225
32.936	24.234	0.765	12.520
29.881	24.065	0.694	11.731
26.924	23.894	0.625	10.929
23.783	23.703	0.552	10.034
20.932	23.525	0.486	9.202
17.76	23.319	0.412	8.235
14.49	23.094	0.336	7.184
11.644	22.886	0.270	6.208
8.492	22.641	0.197	5.061
5.307	22.365	0.123	3.773
2.726	22.100	0.0633	2.532

Table B.3: Adsorption isotherm data for p-xylene at 65 °C

Pressures (mbar)	Total mass (mg)	Relative Pressure (P/Po)	Mass uptake % ((Wt - Wto)/Wto)
0.006	21.121	0.000	0.000
3.366	21.401	0.039	1.334
6.267	21.508	0.074	1.849
9.269	21.591	0.110	2.245
12.351	21.670	0.146	2.629
15.594	21.753	0.185	3.028
18.546	21.827	0.220	3.380
21.546	21.900	0.255	3.732
24.587	21.973	0.291	4.087
27.584	22.046	0.327	4.437
30.553	22.116	0.362	4.772
33.572	22.187	0.398	5.118
36.517	22.255	0.433	5.443
39.53	22.325	0.469	5.782
39.53	22.325	0.469	5.782
38.893	22.311	0.461	5.713
35.934	22.243	0.426	5.386
33.002	22.174	0.391	5.055
29.744	22.093	0.353	4.662
26.923	22.024	0.319	4.329
24.015	21.953	0.285	3.988
20.785	21.868	0.246	3.583
17.864	21.790	0.212	3.207
14.569	21.700	0.172	2.772
11.411	21.608	0.135	2.330
8.174	21.506	0.097	1.840
5.268	21.405	0.062	1.357
2.737	21.303	0.032	0.865

Table B.4: Adsorption isotherm data for m-xylene at 30°C

Pressures (mbar)	Total mass (mg)	Relative Pressure (P/Po)	Mass uptake % ((Wt - Wto)/Wto)
0.013	21.094	0.000	0.000
2.017	21.257	0.134	0.776
3.028	21.309	0.201	1.028
4.034	21.365	0.268	1.292
5.024	21.419	0.333	1.553
5.997	21.471	0.398	1.802
6.997	21.531	0.464	2.215
8.038	21.644	0.534	2.630
8.996	21.692	0.597	2.861
10.003	21.740	0.664	3.088
11.001	21.783	0.731	3.295
11.992	21.823	0.796	3.491
12.997	21.865	0.863	3.689
12.997	21.865	0.863	3.689
11.999	21.846	0.797	3.598
11.005	21.823	0.731	3.486
10.003	21.798	0.664	3.368
9.004	21.773	0.598	3.247
8.001	21.746	0.531	3.117
7.001	21.717	0.465	2.977
5.997	21.686	0.398	2.827
5.007	21.653	0.332	2.666
4.001	21.615	0.265	2.482
3.002	21.570	0.199	2.270

Table B.5: Adsorption isotherm data for m-xylene at 50°C

Pressures (mbar)	Total mass (mg)	Relative Pressure (P/Po)	Mass uptake % ((Wt - Wto)/Wto)
0.01	21.129	0.000	0.000
3.204	21.232	0.076	0.493
6.28	21.393	0.150	1.264
9.487	21.589	0.227	2.200
12.607	21.732	0.302	2.885
15.666	21.858	0.375	3.487
18.621	21.970	0.446	4.023
21.585	22.071	0.517	4.510
24.523	22.173	0.587	4.998
27.547	22.282	0.659	5.520
30.532	22.393	0.731	6.053
33.503	22.500	0.802	6.568
36.593	22.613	0.876	7.110
39.594	22.720	0.948	7.623
39.594	22.720	0.948	7.623
36.013	22.634	0.862	7.209
33.008	22.548	0.790	6.796
29.835	22.455	0.714	6.347
26.935	22.367	0.645	5.923
23.94	22.273	0.573	5.472
20.917	22.174	0.501	5.000
17.919	22.074	0.429	4.520

14.743	21.963	0.353	3.984
11.451	21.839	0.274	3.392
8.154	21.705	0.195	2.748
5.186	21.569	0.124	2.096
2.724	21.432	0.065	1.441

Table B.6: Adsorption isotherm data for m-xylene at 65°C

Pressures (mbar)	Total mass (mg)	Relative Pressure (P/Po)	Mass uptake % ((Wt - Wto)/Wto)
0.004	21.112	0.000	0.000
3.635	21.245	0.044	0.653
6.622	21.348	0.080	1.147
9.658	21.438	0.118	1.580
12.472	21.496	0.152	1.859
15.587	21.552	0.190	2.134
18.442	21.605	0.225	2.389
21.362	21.656	0.261	2.635
24.581	21.713	0.300	2.912
27.402	21.762	0.334	3.149
30.469	21.814	0.372	3.400
33.522	21.866	0.409	3.654
36.567	21.918	0.446	3.902
39.525	21.967	0.483	4.141
39.525	21.967	0.483	4.141
35.935	21.908	0.439	3.855
33.006	21.861	0.403	3.625
30.001	21.809	0.366	3.376
27.009	21.756	0.330	3.120
24.013	21.702	0.293	2.859
20.955	21.647	0.256	2.591
17.934	21.592	0.219	2.325
14.810	21.531	0.180	2.030
11.534	21.463	0.140	1.703
8.188	21.388	0.100	1.340
5.174	21.312	0.063	0.974
2.717	21.240	0.033	0.627

Table B.7: Adsorption isotherm data for x-xylene at 30 °C

Pressures (mbar)	Total mass (mg)	Relative Pressure (P/Po)	Mass uptake % ((Wt - Wto)/Wto)
0.005	21.114	0.000	0.000
2.117	21.445	0.179	1.578
2.996	21.505	0.253	1.864
4.010	21.562	0.339	2.138
5.011	21.616	0.424	2.397
6.018	21.669	0.509	2.648
7.013	21.720	0.594	2.892
8.015	21.770	0.678	3.135
9.035	21.822	0.765	3.384
10.025	21.873	0.849	3.626
10.025	21.873	0.849	3.626
8.992	21.847	0.761	3.503

7.991	21.818	0.676	3.362
6.992	21.787	0.592	3.214
5.995	21.754	0.507	3.052
4.995	21.717	0.423	2.876
3.992	21.675	0.338	2.677
2.985	21.628	0.252	2.448

Table B.8: Adsorption isotherm data for o-xylene at 50 °C

Pressures (mbar)	Total mass (mg)	Relative Pressure (P/Po)	Mass uptake % ((Wt - Wto)/Wto)
0.003	21.106	0.000	0.000
3.648	21.359	0.108	1.212
6.319	21.533	0.187	2.044
9.247	21.744	0.274	3.054
10.644	21.860	0.316	3.606
12.617	22.003	0.374	4.292
15.304	22.199	0.454	5.228
18.211	22.420	0.541	6.282
21.19	22.651	0.629	7.388
24.208	22.892	0.719	8.542
27.203	23.137	0.808	9.710
30.194	23.373	0.897	10.839
32.61	23.558	0.968	11.723
32.61	23.558	0.968	11.723
29.724	23.425	0.883	11.086
26.783	23.266	0.795	10.325
23.736	23.095	0.705	9.505
20.625	22.911	0.612	8.626
17.497	22.721	0.519	7.714
14.703	22.542	0.436	6.858
11.756	22.345	0.349	5.916
8.491	22.111	0.252	4.797
5.256	21.858	0.156	3.592
2.756	21.627	0.081	2.488

Table B.9: Adsorption isotherm data for o-xylene at 65°C

Pressures (mbar)	Total mass (mg)	Relative Pressure (P/Po)	Mass uptake % ((Wt - Wto)/Wto)
0.006	21.118	0.000	0.000
3.645	21.256	0.054	0.663
6.293	21.359	0.093	1.154
9.183	21.470	0.136	1.687
10.662	21.530	0.158	1.973
12.632	21.602	0.188	2.322
15.318	21.699	0.228	2.786
18.147	21.804	0.270	3.287
21.183	21.916	0.315	3.827
24.178	22.027	0.360	4.360
27.162	22.139	0.404	4.897
30.138	22.255	0.449	5.449
33.218	22.371	0.494	6.006
33.218	22.371	0.494	6.006

32.747	22.357	0.487	5.942
29.936	22.276	0.446	5.550
26.938	22.185	0.401	5.115
24.017	22.094	0.357	4.676
20.738	21.990	0.308	4.177
17.604	21.889	0.262	3.694
14.85	21.797	0.221	3.251
11.604	21.685	0.172	2.714
8.471	21.570	0.126	2.163
5.138	21.435	0.076	1.517
2.711	21.320	0.040	0.962

B.2. Adsorption Isotherms Data for Ethylbenzene

Table B.10: Adsorption isotherm data for ethylbenzene at 30 °C

Pressures (mbar)	Total mass (mg)	Relative Pressure (P/Po)	Mass uptake % ((Wt - Wto)/Wto)
0.001	21.107	0.000	0.000
2.015	21.294	0.113	0.896
3.009	21.363	0.169	1.227
4.018	21.430	0.226	1.546
5.009	21.492	0.281	1.841
6.016	21.552	0.338	2.130
7.018	21.611	0.394	2.413
8.022	21.669	0.451	2.691
9.018	21.725	0.507	2.961
10.013	21.781	0.563	3.229
11.024	21.837	0.620	3.494
12.021	21.891	0.676	3.757
13.043	21.947	0.733	4.022
14.026	22.000	0.789	4.277
15.029	22.053	0.845	4.531
16.003	22.105	0.900	4.779
16.003	22.105	0.900	4.779
15.007	22.083	0.844	4.675
14.008	22.056	0.788	4.544
13.008	22.027	0.731	4.405
12.007	21.998	0.675	4.264
11.003	21.967	0.618	4.115
10.004	21.935	0.562	3.961
9.006	21.901	0.506	3.797
8.007	21.866	0.450	3.629
7.007	21.828	0.394	3.446
6.004	21.788	0.337	3.252
5.002	21.743	0.281	3.039
4.003	21.694	0.225	2.803
3.006	21.639	0.169	2.537

Table B.11: Adsorption isotherm data for ethylbenzene at 30 °C (2nd run)

Pressures (mbar)	Total mass (mg)	Relative Pressure (P/Po)	Mass uptake % ((Wt - Wto)/Wto)
0.000	21.103	0.000	0.000
3.002	21.425	0.168	1.526
5.013	21.549	0.282	2.116
7.005	21.662	0.394	2.650
9.004	21.767	0.506	3.148
11.002	21.862	0.618	3.597
13.002	21.949	0.731	4.009
14.995	22.029	0.843	4.388
16.015	22.070	0.900	4.582
16.015	22.070	0.900	4.582
15.001	22.050	0.843	4.490
13.000	22.002	0.731	4.263
11.003	21.950	0.618	4.014
9.004	21.893	0.506	3.744
7.003	21.829	0.393	3.442
5.008	21.756	0.281	3.097
3.003	21.667	0.168	2.673

Table B.12: Adsorption isotherm data for ethylbenzene at 50 °C

Pressures (mbar)	Total mass (mg)	Relative Pressure (P/Po)	Mass uptake % ((Wt - Wto)/Wto)
0.004	21.109	0.000	0.000
3.457	21.687	0.071	2.754
6.593	21.945	0.136	3.990
9.546	22.141	0.198	4.924
12.598	22.300	0.261	5.684
15.509	22.441	0.321	6.360
18.368	22.577	0.381	7.011
21.375	22.720	0.443	7.698
24.354	22.861	0.505	8.372
27.235	22.994	0.565	9.011
30.301	23.135	0.628	9.688
33.337	23.270	0.691	10.333
36.406	23.408	0.755	10.998
39.429	23.542	0.818	11.636
43.116	23.705	0.894	12.419
46.274	23.837	0.960	13.054
46.274	23.837	0.960	13.054
42.021	23.679	0.872	12.296
39.013	23.546	0.809	11.656
36.017	23.414	0.747	11.025
32.953	23.274	0.684	10.351
30.024	23.136	0.623	9.693
26.816	22.981	0.556	8.948
24.004	22.844	0.498	8.293
20.890	22.679	0.433	7.501
17.739	22.501	0.368	6.687
14.739	22.347	0.305	5.914
11.638	22.173	0.241	5.081
8.293	21.965	0.172	4.087

5.215	21.753	0.108	3.071
2.711	21.547	0.056	2.088

Table B.13: Adsorption isotherm data for ethylbenzene at 65 °C

Pressures (mbar)	Total mass (mg)	Relative Pressure (P/Po)	Mass uptake % ((Wt - Wto)/Wto)
0.000	21.103	0.000	0.000
3.164	21.385	0.033	1.334
6.353	21.494	0.068	1.849
9.593	21.577	0.103	2.245
12.584	21.657	0.135	2.629
15.524	21.742	0.166	3.028
18.332	21.817	0.196	3.380
21.298	21.891	0.228	3.732
24.539	21.966	0.263	4.087
27.369	22.040	0.294	4.437
30.538	22.110	0.328	4.772
33.524	22.184	0.360	5.118
36.510	22.252	0.392	5.443
39.382	22.324	0.423	5.782
42.406	22.414	0.455	6.212
45.451	22.485	0.488	6.548
48.487	22.550	0.520	6.856
48.487	22.550	0.520	6.856
44.997	22.483	0.483	6.540
41.998	22.398	0.451	6.135
39.010	22.309	0.419	5.713
35.930	22.240	0.386	5.386
32.947	22.170	0.353	5.055
30.000	22.087	0.322	4.662
27.045	22.017	0.290	4.329
23.999	21.945	0.257	3.988
20.672	21.859	0.222	3.583
17.813	21.780	0.191	3.207
14.641	21.689	0.157	2.772
11.604	21.595	0.124	2.330
8.384	21.492	0.090	1.840
5.391	21.390	0.057	1.357
2.717	21.286	0.029	0.865

APPENDIX C

ADSORPTION ISOTHERMS DATA OF PREVIOUS STUDY ON MCM-41

C.1 Nitrogen adsorption at 77 K

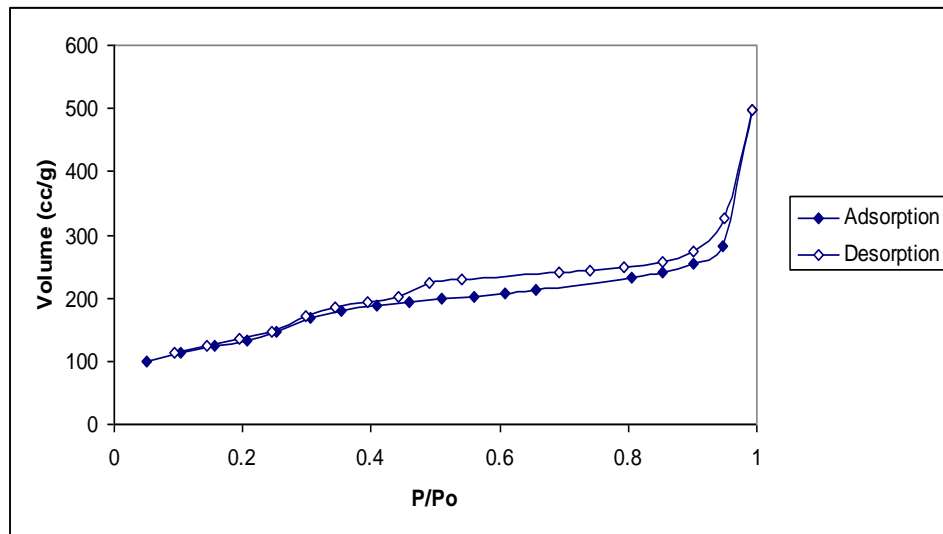


Figure C.1: Nitrogen adsorption at 77 K on MCM-41 in previous study [62]

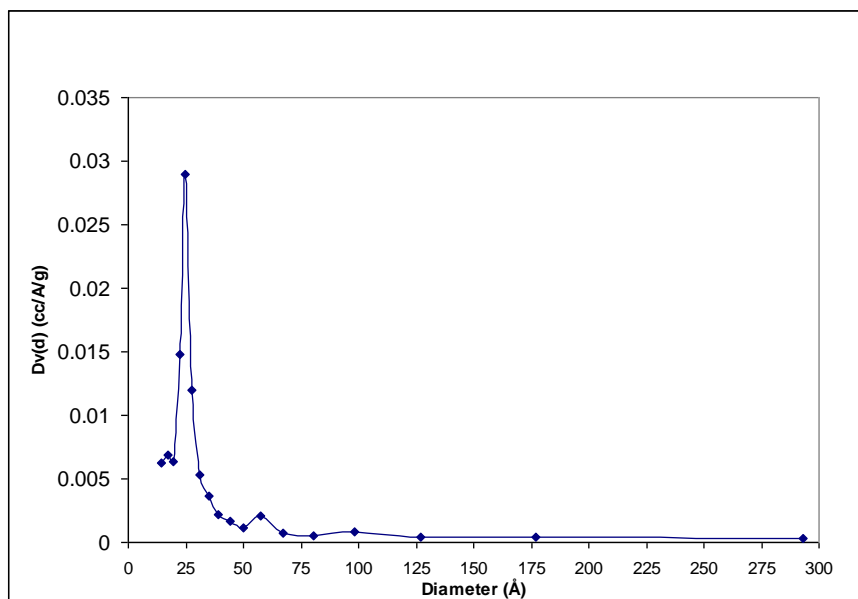


Figure C.2: BJH adsorption pore size distribution of MCM-41 in previous study [62]

BET surface area = 474.5 m²/g
 Pore volume = 0.50 cc/g
 BJH adsorption pore diameter = 2.475 nm

C.2 Equilibrium sorption capacities of C₈ aromatics on MCM-41

Table C.1: Equilibrium sorption capacities for p-xylene [62]

Temperature (°C)	Maximum pressure (mbar)	Total mass (mg)	Maximum relative pressure (P/P ₀)	Mass uptake %
30	14.149	25.104	0.911	24.426
50	39.960	25.471	0.933	25.915
65	41.926	22.967	0.499	17.474

Table C.2: Equilibrium sorption capacities for m-xylene [62]

Temperature (°C)	Maximum pressure (mbar)	Total mass (mg)	Maximum relative pressure (P/P ₀)	Mass uptake %
30	13.944	23.930	0.926	19.570
50	36.623	24.556	0.877	21.308
65	37.616	23.792	0.459	19.170

Table C.3: Equilibrium sorption capacities for o-xylene [62]

Temperature (°C)	Maximum pressure (mbar)	Total mass (mg)	Maximum relative pressure (P/P ₀)	Mass uptake %
30	11.177	25.055	0.946	23.963
50	30.655	24.702	0.910	22.386
65	30.625	24.017	0.456	19.494

Table C.4: Equilibrium sorption capacities for ethylbenzene [62]

Temperature (°C)	Maximum pressure (mbar)	Total mass (mg)	Maximum relative pressure (P/P ₀)	Mass uptake %
30	15.953	24.313	0.897	22.479
65	39.992	23.940	0.429	19.128

APPENDIX D

INTELLIGENT GRAVIMETRIC ANALYZER

D.1. Intelligent gravimetric analyzer (IGA system)

D.1.1. IGA-001- Gas Sorption System

The model IGA-001 system is designed to study the gas sorption properties of materials. This system forms the core of the IGA range of gravimetric analysers. The IGA design integrates precise computer-control and measurement of weight change, pressure and temperature to enable fully automatic and reproducible determination of gas adsorption-desorption isotherms and isobars in diverse operating conditions.

D.1.2. IGA-002 – Vapor Sorption System

The model IGA-002 system is specifically designed to study water and vapour sorption. The system is available in a high vacuum configuration to enable microporous materials to be studied. A selection of pressure sensors enables pressure control at very low partial vapour pressures. The incorporated anti-condensation system extends the temperature range to 50°C over which the full P/P_0 envelope can be measured. This system was used for our work.

D.1.3. IGA-003 –Dynamic Sorption System

The model IGA-003 system is specifically designed for experimental applications where it is necessary to have a dynamic flow of gas past the sample (the determination of multi-component isotherms for example). In this arrangement it is possible to have up to four gas streams mixed prior to entry in to IGA system so that a defined composition is delivered at the sample position.

D.2. Sample Loading

IGA software guides us through the procedure for sample loading. This is initiated either by clicking with the left hand mouse button on the **New sample** tool, which is at the far left of the Tool bar, or by selecting **File, New sample** from the menu. The first stage of the sample loading is to enter the current system password in the message box that will appear after that we select **New sample** tool. The IGA software will be in idle mode after **New sample** tool and our next action will depend on whether we need to reconfigure the IGA system. The sorbate used in the experiment must have corresponding entries in the IGA gas database which is viewed and created by the selection **Setup, Gas** while the IGA is still in idle mode. Sample loading also requires the data for buoyancy corrections which defined in chapter 2 in IGA systems user manual [64].

D.2.1. Gas Setup Tool

Gas setup stores sorbate data but is not used to change sorbate which can only be achieved using **New Application** tool.

When a new sorbate is used the associated physical properties also need to be entered in the IGA gas database and this is achieved by selecting **Setup, Gas** while IGASwin is idling. We can also review and change properties of existing species by selecting the Gas setup button when available during **New Application**. Not all the information is compulsory as some parameters are solely for data reductions and analyses that we may not require. Gas setup is a window with four categories:

1. **General:** which include the name of the sorbate, if it is hazardous or not, chemical name, formula, description and molar mass which is a compulsory parameter.
2. **Compressibility:** at high gas pressure and / or low gas temperature, the buoyancy correction (appendix B in IGA system user manual) is increasingly sensitive to the calculated gas density and therefore to the gas compressibility factor.
3. **Vapour phase:** the distinction between gas and vapour species is defined by the critical temperature which is the first parameter of this category. Any measurement below this temperature may require definition of the vapour pressure, (P_0), for two reasons: firstly, to prevent condensation in the chamber due to over-pressure and, secondly, to enable calculation of relative pressure, P/P_0 at the sample. In the first instance the system will automatically trip if severe condensation occurs since the pressure controller cannot attain the set-point and the failure is equivalent to exhaustion of the sorbate supply and the measurement will stop at this point. If the software calculates, P_0 , from the measured operating conditions then this condition is avoided and, for example during isothermal measurements the scan reverses from adsorption to desorption. This only strictly applies if the saturation vapour pressure is lower than the maximum operating pressure for the current instrument configuration. In the second case the definition of P/P_0 during the measurement and as the fundamental scale for comparing uptake is a normal requirement for measurement of the vapour phase.
The protection against condensation is generally referred to as a part of the IGA "Anti-condensation protection" and operates in conjunction with thermostats and temperature sensors to define and measure the temperature of the chamber. The critical temperature (T_c °C) defines when anti-condensation protection is applied and is the threshold for the vapour pressure calculation using all the other parameters of this category. This is a compulsory parameter for the vapours and will enable the calculations for vapour pressure. The value may also be used in compressibility calculations. The software provides definition by one of three vapour pressure equations. The first equation which is the one we used in our experiments was Antoine equation (see Appendix C)
4. **Sorbate phase:** (Appendix B in IGA system user manual).

D.2.2. New Application Tool

New application changes the IGA configuration in any or all of the following ways:

1. Configuration of the pressure controller (IGA-003, IGA-002)
2. Source of the gas/vapour supply (IGA-002, IGA-002/3)
3. Choice of reactor (and therefore the operating pressure and temperature limit) if more than one option is available.
4. Choice of thermostat if more than one option is available.
5. Definition of the sorbate species and connection of the sorbate supply.
6. Choice of the pressure sensor used for the experiment if IGA has more than one.

If we are about to carry out an experiment for the first time with new sorbate species then first we should check that this species appears in the gas database. If not we should enter the information related to sorbate in the database (see gas setup tool).












The first choice during **New application** tool is the pressure control. For our work the choice is 'static' mode. Which is control of a single component gas or vapour species. Control is not static in most (regulated) application unless the sample is in isothermal equilibrium (i.e., there will be some flow of gas into or out of the IGA chamber to maintain constant pressure).

The second option is the source of gas or vapour species. For our work was liquid reservoir. The third option is the choice of IGA reactor. For our work the selection was SS 316N reactor.

The fourth option is the choice of thermostat. For our work the selection was furnace. Bear in mind that this will set temperature limit for sample pre-treatment and for regeneration for the MCM-41 sample.

Then we should select our sorbate and after that the desired pressure range. For our work which was 100 mbar.

Table D.1: IGA-002 valve Position for static mode gas pressure set (Idle mode)

Valve	Symbol	Position
PIV1		Closed
PIV2 high Pressure Expt.		Closed B Pressure Range P1
PIV2 low Pressure Expt.		Open A Pressure Range P2 Pressure Range P3 Pressure Range Auto
PIV3		Horizontal(closed)
PIV4		Left
PIV5		Up
PIV6		Horizontal(closed)
EV1		Horizontal(closed)
EV2		Vertical(closed)
EV3		Down
Air Admit		Closed

The valves and devices shown in all process schematics within this section are defined as follows:

PIV1	High conductance exhaust valve
PIV2	P2/P3 sensor isolation valve
PIV3	Static-dynamic inlet mode valve
PIV4	Gas-vapour mode valve
PIV5	Static-dynamic exhaust mode valve
PIV6	Counter flow isolation valve
MV1	Admittance control valve
MV2	Exhaust control valve
EV1	Vacuum block-bleed valve
EV2	DSMS isolation valve
EV3	Turbo pump air admittance valve
P1	Primary pressure sensor
P2	Second pressure sensor
P3	Third pressure sensor
LR	Liquid reservoir
V1	IGA vacuum gauge
V2	DSMS vacuum gauge
VENT1	Chamber over-pressure safety valve
VENT2	Liquid reservoir over-pressure safety valve(glass reservoir only)
VENT3	P2/P3 over-pressure safety valve
VENT4	Pump manifold over-pressure safety valve
VENT5	Optional DSMS inlet over-pressure safety valve
D1	DSMS inlet isolation valve
D2	DSMS bypass pump isolation/throttle valve
D3	DSMS auto air admittance valve